



HAL
open science

Low-temperature electrochemistry and spectroelectrochemistry for coordination compounds

Isidoro López, Nicolas Le Poul

► **To cite this version:**

Isidoro López, Nicolas Le Poul. Low-temperature electrochemistry and spectroelectrochemistry for coordination compounds. *Coordination Chemistry Reviews*, 2021, 436, pp.213823. 10.1016/j.ccr.2021.213823 . hal-03188421

HAL Id: hal-03188421

<https://hal.univ-brest.fr/hal-03188421>

Submitted on 10 Mar 2023

HAL is a multi-disciplinary open access archive for the deposit and dissemination of scientific research documents, whether they are published or not. The documents may come from teaching and research institutions in France or abroad, or from public or private research centers.

L'archive ouverte pluridisciplinaire **HAL**, est destinée au dépôt et à la diffusion de documents scientifiques de niveau recherche, publiés ou non, émanant des établissements d'enseignement et de recherche français ou étrangers, des laboratoires publics ou privés.



Distributed under a Creative Commons Attribution - NonCommercial 4.0 International License

Low-temperature electrochemistry and spectroelectrochemistry for coordination compounds

Isidoro López,^{*,‡} and Nicolas Le Poul^{*,‡}

[‡]Laboratoire de Chimie, Electrochimie Moléculaires et Chimie Analytique, UMR CNRS 6521, Université de Bretagne Occidentale, 6 avenue Le Gorgeu, CS93837, 29238 Brest, Cedex 3, France.

Abstract

This review is focused on the current state-of-the art of low-temperature electrochemistry and spectroelectrochemistry applied for coordination and organometallic compounds. From the first tentative steps in the 1960s to the present sophisticated spectroelectrochemical systems, low-temperature studies of redox reactions and coupled chemical processes have always fascinated chemists. The main reason is that low temperature offers the possibility not only to quantify thermodynamics/ kinetics of electron transfer reactions, but also to better decipher mechanistic pathways of chemical-coupled electron transfer reactions. Various cryo-electrochemical and spectroelectrochemical set-ups have been designed leading to significant advancement of *in situ* detection of transient and unstable species generated by electrochemistry. In this review, we detail the novel aspects which can be discovered by performing electrochemical/spectroelectrochemical investigations at low temperature, and the means to carry out resolved electrochemistry at temperatures close to the liquid nitrogen solidification. Specific examples are given to demonstrate the powerful information which can be taken from low-temperature studies for coordination and organometallic chemistry. A conclusion and outlook are also presented to discuss about the perspectives and remaining challenges for this research field.

Contents

1. Introduction	2
1. Low-temperature electrochemistry: technical aspects.....	3
1.2. Low- <i>T</i> electrochemical cells and electrodes.....	5
1.3. Low-temperature supporting electrolytes and solvents.....	9
1.4. Low- <i>T</i> spectroelectrochemical cells.....	12
1.4.1. Thin-layer cryo-spectroelectrochemical cells for UV-vis-NIR and vibrational spectroscopies.....	14
1.4.2. EPR cryo-spectroelectrochemical cells	21
1.4.3. Multi-spectroelectrochemical cells.....	23

2. Low-temperature electrochemistry for coordination or organometallic compounds	24
2.1. Determination of the thermodynamics and kinetics of electron transfer reactions	24
2.2 Mechanistic studies of chemical-coupled electron transfer reactions	28
3. Low-temperature spectroelectrochemistry for coordination or organometallic compounds.....	32
4. Conclusions and outlooks.....	41
Author information.....	42
Notes.....	42
Acknowledgments.....	42
References	42

1. Introduction

Electrochemistry and spectroelectrochemistry have become ubiquitous methods in coordination and organometallic chemistry due to the large amount of data which can be taken from the different redox states of metal and ligands. By comparison to electron transfer (ET) reactions between two redox species, electrochemistry displays the main advantage of directly measuring energetics of the interfacial processes via redox potential values. Another advantage is that it is a time-dependent technique, implying that the timescale of the experiment can be optimized such that kinetics of the chemical processes (electron transfer and/or coupled chemical reaction) can be determined in a straight manner, hence facilitating the elucidation of the reaction mechanisms. Coupling electrochemistry with spectroscopy or microscopy has opened a new area of research, by giving the chance to obtain valuable spectroscopic information of the transient species generated by electrochemical perturbation. First spectroelectrochemical systems were mostly “*ex-situ*”, since the spectroscopic characterization was undertaken after the electrochemical reaction, and mainly from a sample extracted from the electrolyzed solution. More recently, “*in situ*” approaches have been developed, allowing spectroscopic analysis of the solution more/less simultaneously to the electron-transfer reaction. These methods have already become a powerful tool to detect intermediates species of electrode reactions. Thanks to technological progress in spectroscopic instruments (UV, Vis, NIR and IR), “time-resolved” set-ups have progressively emerged as the best strategy to monitor the decay/appearance of the various species generated during the electrochemical processes. The typical timescale for time-resolved measurements lies between several to hundreds of milliseconds. It is fully dependent on the spectroscopic technique, the acquisition/resolution features of the spectrometer, and the electrochemical time constant of the cell. A great majority of spectroelectrochemical set-ups have been designed for absorption spectroscopy, Raman scattering spectroscopy, and electron paramagnetic resonance (EPR). For a few years now, several commercial spectroelectrochemical systems which can afford room-temperature and sub-0°C (typically until -20 °C) UV-Vis-NIR measurements can be

purchased. Spectroelectrochemical systems which involve X-ray absorption spectroscopy (XAS), nuclear magnetic resonance (NMR), and luminescence in the UV or VIS regions have been less developed [1-3].

Room-temperature electrochemical and spectroelectrochemical methods can provide a high quantity of useful information, but these techniques are sometimes limited. This is particularly true when the starting and/or electrochemically-generated species are not stable within the time scale of the experiment. To address this issue, a typical strategy has been to lower the temperature (T) such that the transient species becomes stabilized enough to afford electrochemical and spectroscopic analyses [4]. First electrochemical measurements at low temperatures were officially initiated in the beginning of the 1970s by Van Duyne and co-workers [5], although few studies were previously reported [6-11]. Since these pioneering experiments, low-temperature electrochemistry, coined as “cryo-electrochemistry” when reaching ultra-low temperatures ($T < -80\text{ °C}$ (193 K)), has been used for the structural, thermodynamic and kinetic study of electrode reactions and coupled homogeneous processes. Spectroelectrochemical methods at low- T were concomitantly developed for various spectroscopies (UV-Vis, IR, EPR, Raman...) and a broad panel of cryo-electrochemical and spectroelectrochemical cells were reported.

This review, divided into three sections, aims at describing the different features of low-temperature electrochemistry and spectroelectrochemistry for coordination and organometallic compounds. The first section describes the technical aspects of low- T electrochemistry and spectroelectrochemistry (cells design, supporting electrolyte, solvents, and electrodes). It is particularly focused on the different models which have been designed for UV-Vis-NIR, IR and EPR spectroelectrochemical cells which could be of help for studies in coordination chemistry. The second section concerns literature examples of low-temperature electrochemistry of organometallic and coordination compounds, including both determination of the thermodynamics/ kinetics of electron transfer reactions, as well as mechanistic studies of chemical-coupled electron transfer reactions by characterization of transient species. The third section gives insights into cryo-spectroelectrochemistry, with specific examples of low- T spectroelectrochemical studies for coordination / organometallic compounds. The review is completed by a conclusion part which condenses the main information to be taken from the previous sections, and gives future perspectives which can be envisaged from the state of the art.

1. Low-temperature electrochemistry: technical aspects

The development of cryo-electrochemical and cryo-spectroelectrochemical measurements has been for a long time hindered by the large number of technical problems associated to the low temperature (solvent freezing, ohmic drop, precipitation...). Improvement of the liquid electrolytes and mixtures of solvents, as well as low current devices in the 1970s has allowed the emergence of this new research area.

1.1. Cooling systems

Two main approaches have been developed so far to cool electrochemical cells (Figure 1): (i) immersion in the coolant, or (ii) flowing the coolant through a specific cell jacket. Simple immersion in slush baths or salt-ice mixtures such as dry ice in acetone, or cooled ethanol (193 K) is the most practical, and probably the most used, but often does not allow any accurate control of the temperature (Figure 1A). Moreover, heat exchange with the surroundings is hard to avoid over long-time experiments and the temperature of the bath cannot be varied intentionally. Jacketed cells in which the coolant flows according to a defined flux to allow thermal equilibrium was shown to be more interesting in many aspects (Figure 1B). Indeed, such cooling system offers the advantage of stabilizing the temperature (no relative heat transfer with surroundings). In addition, the temperature can be tuned by controlling the heating power of the cooler of the refrigerated bath. Coolants such as methanol or 2-propanol are the usual solvents used to achieve temperatures down to 193 K. However, the main limitations are the freezing point of the coolant, as well as the high energy/power necessary to cool the bath at temperatures below 183 K. Moreover, insulation of the tubes connecting the circulator to the cell is hard to accomplish. Fortunately, swapping from organic solvents to liquid nitrogen as coolant has knocked down the barriers to perform ultra-low-temperature electrochemical studies. Such systems have been well developed on the basis of liquid-nitrogen cryostats which are commercially available nowadays. Briefly, the principle is to inject chilled liquid nitrogen to the cell at a specific flow rate such that the rate of cooling equals the rate of warming of the cell by its surroundings. In order to finely tune the temperature, the liquid nitrogen is pre-passed over a resistance heater which is controlled in a feedback mode using the signal from a thermocouple positioned in close proximity to the cell. One drawback of this system is the poor thermal conductivity of N_2 ($0.09 \text{ mW cm}^{-1} \text{ K}^{-1}$ at 100 K) which is in the same order of typical isolators. Accordingly, the electrochemical cell can take several ten of minutes before reaching the thermal equilibrium with the cryogenic fluid.

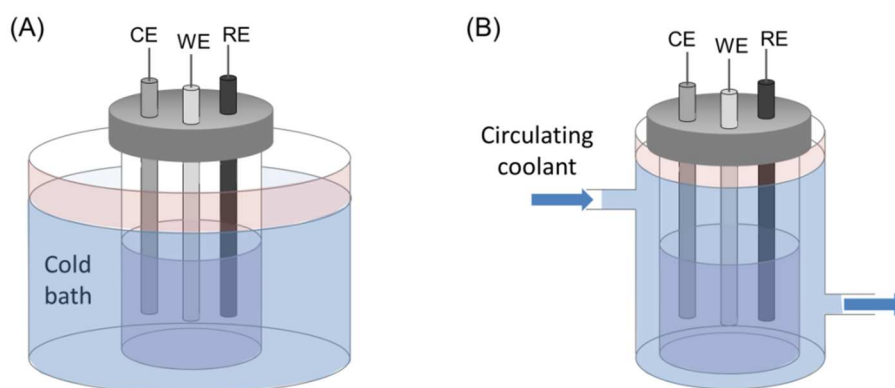


Figure 1. A) Static and B) dynamic cooling systems for electrochemical cells. CE : Counter electrode; WE: Working electrode; RE : Reference electrode.

1.2. Low-*T* electrochemical cells and electrodes

Low-temperature electrochemical cells are usually designed according to the cooling system used as discussed above. For simple immersion, low-temperature cells are similar to room-temperature models but often modified with an elongated cell body such that dipping of the working electrode compartment in the coolant is facilitated. For jacketed cooling systems based on refrigerated organic solvents such as methanol or propanol, high volume (>10 mL) cells are usually constructed to improve temperature stability. They are typically made of glass but Teflon and polyethylene can be used in certain cases [12]. When liquid nitrogen is used as coolant in a cryostat, low volume (2 mL or less) cells are needed to achieve fast thermal equilibrium.

Chronologically, first electrochemical measurements were performed with cells immersed in the coolant at a fixed temperature [10, 11]. Later on, in 1972, van Duyne and Reilley [5] proposed a different cell design for allowing measurements at variable temperatures: a 3-electrodes cell characterized by uniform current and potential distributions across the surface of the working electrode and short inter-electrodes distances for lowering solution resistance effects was inserted in a vacuum jacketed dewar. Cooling of the cell was achieved by sequential flowing of compressed, dry nitrogen gas through a copper coil immersed in a liquid nitrogen heat exchanger and the dewar. This cryostated cell was tested successfully in the 90-300 K temperature range. In 1983, Nagaoka and Okazaki improved van Duyne's cell by decreasing cryostat size and by regulating the nitrogen gas flow rate through adjustment of the switching frequency of the heater [13]. In the late 1980s, the discovery of HTSCs (high-temperature superconductors) gave more impetus on the search for ultra-low temperatures electrochemical apparatus. Aiming at performing electrochemical measurements with HTSCs electrodes, Murray *et al.* designed a cell which could fit a slotted stainless steel sleeve that included a cylindrical epoxy assembly (containing both working and references electrodes) as well as a coplanar auxiliary electrode at the bottom [14, 15]. Working electrodes were initially of micrometer size to decrease solution resistance effects. Moreover, the separation between the working and counter electrodes was kept at minimum distance (0.5 mm). The electrochemical cell was directly placed into a liquid nitrogen cryostat or bolted directly to the cold finger of a helium refrigerator cryostat before cooling down. Measurements were made either with glass [14] or aluminum cells [15]. Concomitantly, Green *et al.* developed cryoelectrochemical cells which could accommodate HTSC/metal micro- and macro-sized electrodes (Figure 2) [16-18]. Cryo-robust epoxy assemblies were particularly shown to be versatile and resistant over long periods to chlorinated solvents at low temperatures [19]. This type of cell was more recently improved by enabling easy removing of all components from the glass cell, thus allowing perfect cleaning of the cell and electrodes [20].

An alternative strategy for low-temperature electrochemical experiments in aqueous solution was recently reported [21]. The system is based on a "supercooled" electrode (gold wire). Cooling the working electrode with liquid nitrogen on the top creates a circular region of 60 μm at low and

relatively constant temperature around the electrode surface in the liquid electrolyte. This system was shown to be interesting for low-temperature (260 K) studies of enzymes.

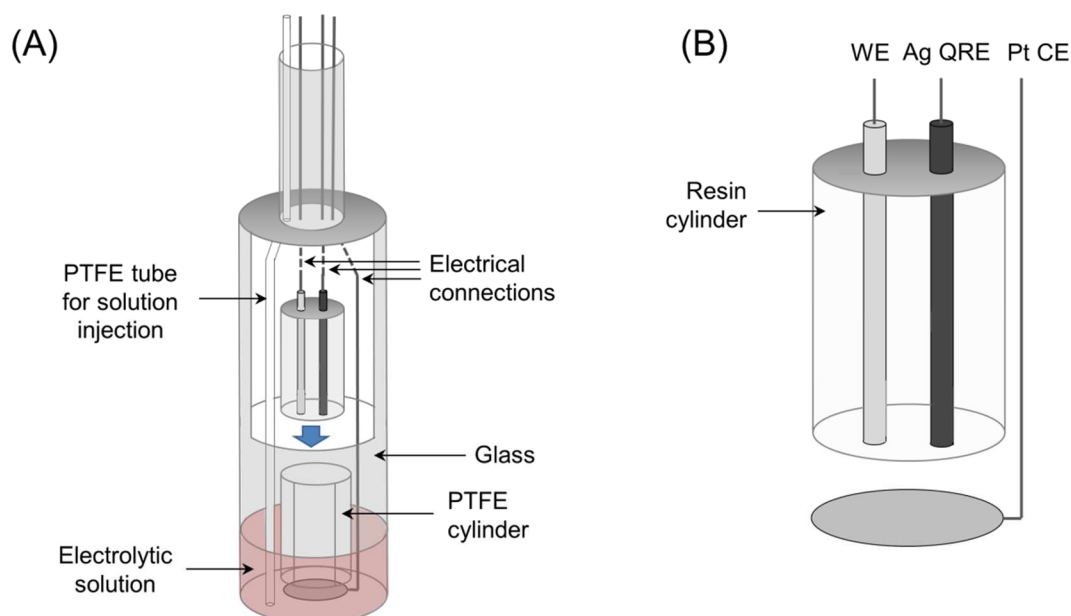


Figure 2. A) Variable-temperature cryoelectrochemical cell and B) two-electrode assembly developed by Green *et al.* [20].

Various materials have been used as working electrodes at low temperatures. In the metal series, most of measurements have been performed with gold or platinum, because of their good intrinsic conductivity at low temperature (less lattice vibrations), which make them as usable as at room temperatures. Several experiments have also been performed with solid mercury [13, 22-27]. In that specific case, the main interest was to take advantage from the highly negative potential limit in comparison to Pt or Au. Electron-transfer properties of metallic electrodes modified with self-assembled monolayers [14, 28-30] or more rarely a redox-polymer [31] were also evaluated at low temperatures. A great advantage of this approach is a simplification in the analysis of the results as mass-transfer processes do not play a significant role except for the diffusion of counterions. Several low-temperature experiments have also been carried out with glassy carbon working electrodes [32-37] and HTSCs at solid state [38, 39], or with liquid electrolytes [16, 18, 19, 40-43]. More recently, several studies reported surface modification of HTSC electrodes, using self-assembled monolayers (SAMs) [44, 45] or conducting polymer [46] that incorporated a redox probe such as ferrocene.

Solution resistance is a major problem in low temperature electrochemical measurements and analysis. The “*iR* drop”, i.e. voltage perturbation due to solution resistance, is governed by the cell current and the effective resistance between the working and reference electrodes. Even if current densities decrease with temperature due to lower diffusion of the species, it does not cancel the *iR* drop effect.

In consequence, specific choices concerning the electrodes design are necessary. Two main solutions have been proposed so far: decrease of working electrode area and/or decrease of working-reference electrodes distance. The use of ultramicroelectrodes (rad. $< 10 \mu\text{m}$) or microband at very low temperatures ($T < 180 \text{ K}$) has been initially preferred considering that the iR drop is intrinsically lower with microelectrodes (the surface area, thus the current, is radius dependent in a square manner) [16, 27, 31, 40, 47, 48]. Another advantage of ultramicroelectrodes is the enhancement of the mass-transfer at the periphery of the electrode, thus increasing the faradic/capacitive current ratio, in comparison to macroelectrodes. However, one main inconvenient is that microelectrodes require low-current detectors and noise-isolated equipment (Faraday cage). The use of macroelectrodes (typically $> 0.05 \text{ cm}^2$) for low temperature measurements has however become possible with the discovery of electrolytic solutions with low solution resistance [5, 17, 31]. The problem of solution resistance was also partially solved by decreasing the distance between the working electrode and the reference electrode. This could be obtained by introducing a Luggin capillary in close proximity to the working electrode [5, 49, 50]. Also, low-sized epoxy-based cryo-robust cylindrical containers which can embed two or three electrodes in close distance (1 mm) can be used to minimize the iR drop. This approach was for instance well developed by Murray [14, 15] and Green [20] for the study of electron transfer reactions at 100-120 K. One main advantage of such system is the possibility to tune the nature (metal, glassy carbon, HTSC...) and/or size of the electrodes.

Many low-temperature electrochemical experiments have been performed with aqueous references electrodes kept at room temperature. Hence, in an initial proposal, van Duyne and Reilley used a SCE reference electrode which is in contact with the low-temperature solution through an intermediate non-aqueous salt bridge and a Luggin capillary probe [5]. The intermediate salt bridge played two roles: protection against contamination of the non-aqueous sample solution by water from the reference electrode, and thermal isolation of the SCE from the low-temperature environment. Reference electrode probe-working electrode spacing was adjustable (1 mm is usual) and the spherical joint permitted precise electrode alignment. This approach has also been extended to external organic reference electrodes such as Ag/AgNO_3 in PrCN [22, 51] or a Pt wire in a Fc^+/Fc equimolar electrolytic solution [52]. In these cases, the reference was housed in a distinct compartment separated from the cell solution compartment by a porous frit. For the ferrocene-based system, the compartment was sealed and protected from air to avoid both the introduction of humidity in the cell and the degradation of the ferrocenium ions. Obviously, this strategy is less convenient when the electrochemical solution and its surrounding environment need to be strictly air-tight, because of highly sensitive compounds. In that case, silver or platinum wires can serve as a quasi-reference electrode, the "real" redox potential being adjusted by addition of a standard redox couple such as ferrocene at the end of the experiment [53]. This strategy is very convenient when the sample space is

minimal as occurring in cryostats even if they provide only approximate measurements of the potentials.

For electrochemistry in frozen aqueous solutions, different approaches were developed [48, 54-57]: for example, measurements in frozen saturated LiCl aqueous solution (170 K) were performed with an Ag/AgCl/LiCl reference electrode that was kept externally at room temperature and connected to the cell via a salt bridge [58].

Despite the different possibilities of combination presented above, the measurement of the “real” potential for the redox species in solution is challenging. The first problem arises from the Soret effect, i.e. thermal migration of species due to the temperature gradient within the cell. Hence, strong electrolytes will concentrate in the cold region, causing a change in electrode potentials in the order of hundredths of a millivolt per degree. However, this effect can be neglected when the reference electrode/bridge compartment is removed during temperature changes. A second issue, which must be considered, is the thermal liquid junction potential in nonaqueous media due to precipitation at the bridge junction, thus introducing an uncompensated resistance and a significant potential change. At last, since the standard potential E^0 of a redox couple is proportional to the free energy change accompanying the electron transfer, it shifts with the temperature following the relationship $nF(\Delta E^0) = T\Delta S^0 - \Delta H^0$ if it is immersed into the sample solution (n is the number of electrons, F the Faraday constant, ΔS^0 is the standard entropy of reaction, ΔH^0 is the standard enthalpy of reaction). Thus, knowledge of the entropic term appears as determining for adjustment of potential values. Furthermore, decrease of temperature can lead to a significant change of concentrations of the species involved in the redox process of the reference electrode resulting in an additional change of the equilibrium potential. These two phenomena seem favor the employment of compartmentalized reference electrodes kept thermostated around room temperature to carry out cryo-electrochemistry.

1.3. Low-temperature supporting electrolytes and solvents

The first question that usually arises when considering a low-temperature experiment is the choice of solvent and supporting electrolyte. The freezing point of water limits the lowest practical temperatures for studies in fluid aqueous solution to values near 0 °C. Of course, the freezing point of concentrated aqueous salt solutions is considerably depressed so such systems could be used as fluid electrolytes at lower temperatures, but this is not commonly done [54, 55, 57]. It is much more popular to use non-aqueous solvents for low-temperature studies. There are two motivations, the more common of which is the desire to make measurements down to the lowest temperature possible using a solvent/supporting electrolyte system compatible with the chemical properties of the compounds to be studied. In other instances, the purpose of the experiments is to study the effect of solvent on a temperature-sensitive parameter (e.g., a heterogeneous electron-transfer rate constant), thus a variety of solvents is sought in which low-temperature measurements can be made.

Different approaches have been explored in the literature to obtain ionic conductivity media allowing for performing good electrochemical measurements at very low temperatures. For instance, it has been proposed the use of frozen aqueous electrolytes such as $\text{HClO}_4 \cdot 5.5 \text{H}_2\text{O}$ whose conductivity is explained by the movement of protons along the lattice structure as a result of water molecule reorientation and hydrogen bond breaking processes [54, 55]. Another strategy consists in the use of inorganic solid electrolytes like RbAg_4I_5 or $\text{Ag} \beta''$ -alumina which display good ionic conductivity at very low temperature [59-62]. However, the redox process studied in these electrolytes is limited to the reduction/oxidation of silver.

A more interesting approach for the evaluation of the electrochemical properties of coordination and organometallic compounds is the utilization of organic liquid electrolytes which can dissolve electroactive molecules and provide decent ionic conductivities to carry out the experiments. Fortunately, a few common solvents employed in the study of the redox properties of transition metal complexes at room temperature are also suited for measurements at very low temperatures ($T \leq -80$ °C). Probably, the most attractive examples are CH_2Cl_2 and acetone solutions containing 0.05 M of tetraalkyl ammonium hexafluorophosphate or perchlorate salts as supporting electrolyte. As it will be shown in sections 2 and 3, these two electrolyte systems have been successfully used for cryo-electrochemical and spectroelectrochemical measurements on coordination compounds. Acetonitrile is another traditional non-aqueous solvent widely used for experiments at room temperature. It presents the advantages of a high dielectric constant and excellent solubility of common supporting electrolytes; however, the lowest attainable temperature with this media is around -40 °C, which is not enough for the scope of numerous studies. Interesting alternatives to acetonitrile are propionitrile and butyronitrile as these two solvents exhibit only slightly worse dielectric and solubility properties but much lower melting points (-92 °C and -112 °C, respectively). Surprisingly, cryo-electrochemical studies on transition metal complexes exploiting these electrolytes are scarce in the literature. An explanation could be their enhanced toxicity as compared to the associated to other common solvents which can also be employed at ultra-low temperatures.

There has been, over the years, a strong research competition for finding a liquid electrolyte allowing for carrying out a reliable electrochemical measurement at the lowest possible temperature. A fundamental motivation for this work is the discovery of a medium enabling the analysis of the electrochemical behavior of an electrode made of a HTSC material in the vicinity of its critical temperature (T_c). In this context, the lowest temperature for any electrochemical measurement with liquid electrolyte was reported by Murray and co-workers [63]. They developed electrolyte solutions based on chloroethane/butyronitrile solvent mixtures. Their strategy was to examine combinations of low-melting liquids with relatively high dielectric constant and low viscosity. Butyronitrile has a large dielectric constant whereas chloroethane (a gas at room temperature) has a low melting point and a

low viscosity. With a 1:1 volume ratio mixture of these two solvents, containing tetrabutylammonium perchlorate as supporting electrolyte (0.2 M), they successfully recorded CV curves for freely diffusing tetracyanoquinodimethane (TCNQ) on a gold microband electrode at 88 K. Below this temperature, the faradaic/capacitive currents ratio becomes too low for any possible analysis. Since this record, different mixtures have been tested, changing solvents and supporting salts [16, 17]. The application of these exotic liquid electrolytes to the electrochemical and spectroelectrochemical study of coordination and organometallic compounds remains to be explored. Importantly, the reached ultra-low temperatures could allow for detecting and stabilizing extremely short-living key reaction intermediates.

Table 1 and Table 2 summarize several combinations of solvents and supporting salts used as liquid electrolytes in low temperature studies. The usual proportions used for cryo-electrochemistry are approximately 10^{-3} M of the electroactive species and 10^{-1} M of the supporting electrolyte, as typically used for room temperature analysis. The increase of concentration in supporting electrolyte was shown to have for most of the time beneficial effects on both molar conductivity and freezing point in aprotic solvents.

Table 1. Lowest temperature attainable for liquid electrolytes involving no mixture of solvents

Solvent	Electrolyte	Lowest T/K	Ref.
Acetone	NEt ₄ ClO ₄ (saturated)	198	[64]
	0.30 M NEt ₄ PF ₆	198	[47]
	0.10 M NBu ₄ ClO ₄	206	[65]
Acetonitrile (MeCN)	0.30 M NBu ₄ PF ₆	258	[47]
	0.10 M NBu ₄ ClO ₄	228	[66]
	0.10 M NEt ₄ ClO ₄	228	[5]
	0.10, 0.30, and 0.60 M NBu ₄ PF ₆ and NBu ₄ ClO ₄	233	[27]
	0.20 M NBu ₄ PF ₆	228	[31]
Benzonitrile (PhCN)	0.10 M NEt ₄ ClO ₄	273	[67]
	0.10 M NBu ₄ ClO ₄	273	[67]
	0.10 M NOct ₄ ClO ₄	273	[67]
Butyronitrile (PrCN)	0.30 M NBu ₄ PF ₆	198	[47]
	0.20 M NBu ₄ PF ₆	173	[31]
	0.10 M NBu ₄ ClO ₄	168	[5]
	0.30 M NBu ₄ ClO ₄	143	[22]
	0.10, 0.30, and 0.60 M NBu ₄ PF ₆ and NBu ₄ ClO ₄	193	[27]
1,2-Dichloroethane (DCE)	0.10 M NBu ₄ ClO ₄	243	[67]
Dichloromethane (DCM)	0.05 M NBu ₄ ClO ₄	183	[33]
	0.05 M NBu ₄ PF ₆ , NBu ₄ BF ₄ or NBu ₄ SO ₃ CF ₃	183	[33]

	0.10 M NBu ₄ ClO ₄	188	[68]
	0.10 M NBu ₄ ClO ₄	223	[67]
	0.10 M NBu ₄ PF ₆	208	[69]
	0.10 M NBu ₄ Cl	182	[70]
1,2-Dimethoxyethane (DME)	NBu ₄ PF ₆	213	[71]
<i>N,N</i> -Dimethylformamide (DMF)	0.10 M NBu ₄ ClO ₄	195	[5]
	0.10 M NEt ₄ ClO ₄	213	[51]
	0.30 M NBu ₄ PF ₆	223	[25]
	0.10, 0.30, and 0.60 M NBu ₄ PF ₆ and NBu ₄ ClO ₄	213	[27]
Ethanol (EtOH)	0.10 M LiClO ₄	193	[72]
	0.50 M LiClO ₄	168	[5]
Methanol (MeOH)	0.10 M LiClO ₄	213	[72]
	1.00 M LiClO ₄	183	[5]
1-Propanol (1-PrOH)	0.10 M LiClO ₄	213	[72]
2-Propanol (2-PrOH)	0.10 M LiClO ₄	193	[5]
Propionitrile (EtCN)	0.30 M NBu ₄ PF ₆	198	[47]
	0.20 M NBu ₄ PF ₆	183	[31]
	0.10 M NBu ₄ PF ₆	197	[73]
	0.10 M NBu ₄ ClO ₄	173	[5]
Pyridine	0.10 M NEt ₄ ClO ₄	243	[67]
	0.10 M NBu ₄ ClO ₄	243	[67]
	0.10 M NOct ₄ ClO ₄	243	[67]
Tetrahydrofuran (THF)	0.10 M NBu ₄ ClO ₄	192	[74]
	0.2 M NBu ₄ ClO ₄	195	[75]
	0.10 M NBu ₄ PF ₆	197	[73]
NH ₃	0.10 M KI	203	[76]
	0.03 M LiCl	213	[77]

Table 2. Lowest temperature attainable for liquid electrolytes involving mixture of solvents

Mixed solvents	Electrolyte	Lowest <i>T</i> /K	Ref.
DMF/MeOH (1:1 and 2:3)	0.2 M NBu ₄ BF ₄	193	[78]
DCM/CF ₃ CO ₂ H/(CF ₃ CO) ₂ O (20: 1:1)	0.2 M NBu ₄ BF ₄	195	[79]
DCM/MeCN (1:1)	0.5 M NBu ₄ Cl	188	[69]
PrCN/EtCN (69:31 wt %)	0.1 M NBu ₄ ClO ₄	155	[5]
PrCN/EtBr (1:1))	0.2 M NBu ₄ ClO ₄	128	[63]
PrCN/EtBr/isopentane/methylcyclopentane (2:2:1:1)	0.2 M NBu ₄ ClO ₄	115	[63]
PrCN/EtCl (1:1)	0.2 M NBu ₄ ClO ₄	88	[63]
PrCN/EtCl (1:2)	0.2 M NBu ₄ PF ₆	95	[31]
MeCN/toluene (1:5.4)	0.1 M NBu ₄ PF ₆	263	[80]
DMF/ toluene (2:3)	0.1 M NEt ₄ PF ₆	185	[81]

DMF/ toluene (1:1)	0.1 M NBu ₄ PF ₆	213	[81]
EtCl/THF/2-MeTHF (16:7:1)	0.60 M LiBF ₄	99.5	[17]
EtCl/THF (2:1)	0.60 M LiBF ₄	102	[16]

1.4. Low-*T* spectroelectrochemical cells

In this section, we provide an overview of relevant experimental approaches to perform cryo-spectroelectrochemical measurements along with a discussion on the valuable information extracted from these techniques for diverse compounds. As for electrochemical equipment, the design of spectroelectrochemical cells for experiments at very low temperatures is more challenging than that found in conventional devices working at room temperature. The same technical considerations previously discussed must be addressed for the implementation of a reliable cooling system, the prevention of air and moisture entries and the appropriate choice of liquid electrolytes.

At first instance, the simplest approach to carry out a cryo-spectroelectrochemical experiment is the exhaustive oxidation or reduction of a solution of the studied molecule by potential-controlled bulk electrolysis and the monitoring of the electrochemical process in real-time with an optical fiber probe or another detection mode. Such approach is commonly reported for room-temperature studies when redox species generated by electrolysis are stable over minutes/hours [82-85]. However, this configuration is unpractical at low temperature because bulk electrolysis can last several hours as a consequence of the decrease of the heterogeneous electron transfer constant and the increase of the viscosity of the solution which slows down the forced mass transfer of the electroactive species.

One strategy to optimize the electrolysis time has been to decrease the volume of electrochemical cells while keeping a sufficiently large working electrode area such that exhaustive electrolysis of the solution could occur more rapidly. For instance, Czernuszewicz *et al.* were among the first to develop a small volume (1.5 mL) cryo-spectroelectrochemical cell based on exhaustive electrolysis to record the Raman spectrum of a Fe(IV)=O porphyrin complex at low temperature (233 K) [86]. A Pt gauze basket (12 mm diameter, 15 mm height) suspended above a stirring bar was used as working electrode. Small volume (mL) spectroelectrochemical cells were also widely developed for EPR measurements in the 1980s. For example, Bond and co-workers reported a 0.2 mL cell which could be used for EPR measurements at low *T* [87] (see section 1.4.2 for details). The electrochemical response of the cell at room and low temperatures were evaluated by recording the CVs of various organometallic and organic molecules. Although the shape of CV curves obtained at room temperature were identical to the one recorded in common and larger volume electrochemical cells, the CVs were severely distorted at very low temperature as a consequence of an increase in the *iR* drop and/or transition from a semi-infinite diffusion to a thin layer regime. Moreover, the span of the experiment to achieve an EPR signal was reaching several minutes.

A more attractive approach to develop cryo-spectroelectrochemical cells is the use of thin layer electrochemistry (TLE). Spectroelectrochemical methods based on TLE have been widely carried out at room and very low temperatures. In TLE, a small volume of the solution containing the electroactive molecule and the supporting electrolyte is confined between the electrode surface and an optically transparent material such as quartz or calcium fluoride windows. Electrochemical methods like low scan rate cyclic voltammetry and chronoamperometry are then performed within this sandwiched and thin liquid layer. Since the electrode surface/volume of solution ratio is extremely high in this configuration, the full oxidation or reduction of electroactive species enclosed in the thin layer occurs in a few seconds, even at very low temperatures. Consequently, the fast spectroscopic changes triggered by electrochemistry can be monitored with the convenient instrumentation. From a simple view, spectroelectrochemical methods based on TLE exploit the possibility of achieving exhaustive bulk electrolysis in a few seconds within the thin layer. This aspect represents a remarkable advantage in experiments at very low temperatures, since conventional bulk electrolysis under that conditions are extremely long as it was discussed above. Thus, thin layer cryo-spectroelectrochemistry offers the opportunity of recording the optical properties of reduced/oxidized species which are unstable in the timescale of minutes at very low temperatures.

Despite the practical benefits of the TLE approach, two serious drawbacks must be noted. From a spectroscopic viewpoint, the detected signal is small as a consequence of the low amount of electroactive molecule contained in the thin layer. Therefore, reliable measurements demand instrumentation featuring remarkable sensitivity which is relatively expensive. Alternatively, high concentration in redox species can be used, but may lead to lower solubility and possible aggregation of compounds. Concerning the electrochemical aspects, the detrimental iR drop effect is exacerbated because the working electrode is geometrically more isolated from the reference electrode than in common large volume electrochemical cells. The increased ohmic drop can induce a substantial difference between the applied and the actual potentials of the working electrode, as well as the emergence of a non-uniform current distribution on the surface of the working electrode. Nevertheless, most of the designs for cryo-spectroelectrochemical cells discussed in this review seem to have successfully minimized iR drop effects and the adopted strategy has been the same: placing a pseudo-reference electrode near to the thin layer.

In the next sections, we have split our discussion into two differentiated blocks. First, a critical description of the most relevant cryo-spectroelectrochemical cells designed for UV-Vis-NIR and IR/Raman spectroscopies is provided. It follows a second block in which the devices developed for electron paramagnetic resonance (EPR) measurements are reviewed. Overall, we think that fundamental differences in the experimental approach to conceive and implement these two kinds of cells justify the separated discussion.

1.4.1. Thin-layer cryo-spectroelectrochemical cells for UV-vis-NIR and vibrational spectroscopies.

Two different approaches can be envisaged for constructing thin layer cryo-spectroelectrochemical cells compatible with UV-vis-NIR and vibrational methods depending on the pathway of the detected radiation: transmission and reflection cells. We will discuss separately the reported designs for these two configurations in the next sub-sections, highlighting their associated advantages and inconveniences.

1.4.1.1. Low-temperature transmission thin-layer cells.

In transmission spectroelectrochemical cells, the use of an optically transparent electrode (OTE) allows to recover the photon flux traversing an optically transparent window, the thin layer and the working electrode. The relative orientation between incident light and detector corresponds to the geometry adopted in common and commercially available spectrophotometers for sample solution analysis in quartz cuvettes. Since OTE are employed as working electrodes, these devices are known as optically transparent thin layer electrochemical (OTTLE) cells [88]. Two different types of working electrodes, transparent or perforated, are commonly used for such cells:

On one hand, doped fluoride (FTO) and indium (ITO) tin oxide materials deposited as thin films (typically 10-100 nm) on quartz/glass/polymer surfaces are amongst the most common transparent electrodes used in transmittance mode at room temperature in the visible domain [1, 2]. Alternatively, boron-doped diamond (BDD) films (500-1000 nm) deposited on quartz have shown to be also suitable transparent electrodes for both UV-Vis and IR spectroelectrochemical studies. When compared to tin oxide materials, BDD-based OTEs display wider potential and spectral ranges, as well as better inertness to chemically aggressive environments. Many examples of room-temperature spectroelectrochemical studies using tin oxide and BDD transparent materials have been reported, but no study has been described for low-temperature conditions so far. One probable reason is the low intrinsic conductivity of these materials (for instance $R = 10^{-4} \Omega\cdot\text{cm}$ for ITO and $10^{-2} \Omega\cdot\text{cm}$ for BDD) which may contribute to the distortion of the current-potential curves at low temperatures in resistive media.

On the other hand, metal grids, such as Pt, Au, Ag and Ni have been widely used for OTTLE cells at room and low temperatures. The density of the grid, varying between 30 to 1000 wires per cm, is usually optimized to allow fast electrolysis as well as good transmission of the optical signal. Various setups of low- T OTTLE cells have been designed since the 1990s. For example, Sweigart and co-workers adapted a room-temperature model (Figure 3B) [89] to achieve *in situ* spectroelectrochemical measurements down to 238 K in acetonitrile [66]. Cooling of the solution was achieved by an external frame made of Teflon shrink tubing. Pin holes were made in the shrink tubing so that chilled nitrogen gas flew out onto the salt plates in the middle of the frame. A thermocouple was inserted between the

cell windows and the cooling frame to monitor the temperature. Another interesting model of OTTLE cell was developed by Lexa and co-workers through the combination of a previously-reported room-temperature spectroelectrochemical cell [90] and a set-up proposed by Duff and Heath [91]. It consisted of a simple spectroscopic quartz cuvette (0.5 mm thickness) with a double jacket, surmounted by a sealed glass compartment (Figure 3A). The Pt mesh working electrode was introduced in the narrow part of the cell, whereas the reference (Ag/AgCl in DMF/NBu₄Cl/NBu₄ClO₄) and the Pt counter electrodes lied in the upper part. The control of the temperature was carried out by circulation of isopropanol with the help of a cryostat within the quartz double-jacketed space. A similar in-house spectroelectrochemical cell was designed by Fujii and co-workers in 2011 for the study of iron-porphyrins [92]. The cell was placed in a low-temperature chamber set on a spectrometer and cooled to low temperature (193 K).

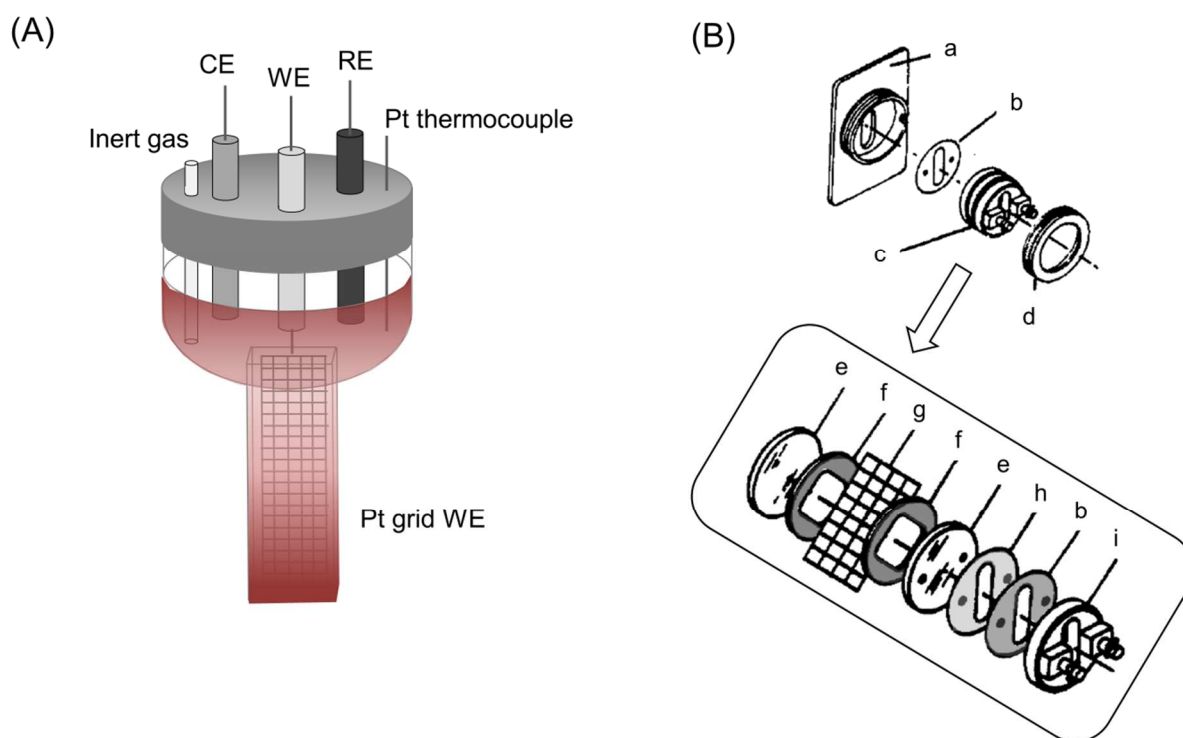


Figure 3. A) Low-temperature UV-Vis OTTLE spectroelectrochemical cell developed by Lexa *et al.* [90]. B) IR OTTLE spectroelectrochemical cell model developed by Mann *et al.* [89] for room temperature measurements and further modified by Sweigart and co-workers [66] for low-*T* studies. (a) back plate, (b) Teflon gasket, (c) salt plate/minigrad electrode assembly, (d) knurled end cap, (e) NaCl salt plates, (f) Tefzel gaskets, (g) gold minigrad electrode, (h) indium gasket, (i) needle plate. Reprinted with permission from [89], copyright (1987) American Chemical Society.

A sophisticated model of cryo-OTTLE cell was alternatively proposed by Hartl and co-workers in 1994 [93] on the basis of a room-temperature system described a few years before [94]. The full low-*T*

set-up mainly consists of a liquid-nitrogen cryostat displaying crossed pairs of CaF₂ (IR) or quartz (UV-VIS) windows at the bottom, and a spectroelectrochemical cell (containing also CaF₂ windows) placed into the inner chamber of the cryostat in a close contact with the heat/cold exchanger. As shown in Figure 4 for the low-temperature cell, the Pt (or Au) working and Pt auxiliary minigrad electrodes are melt-sealed in an insulating polyethylene spacer, together with a silver pseudo-reference wire. Diffusion of electrogenerated species between the working and auxiliary electrodes was shown to be negligible on the experimental timescale (seconds), especially at low temperatures. The spacer is then fixed between two CaF₂ windows kept in position with screws to compensate for thermal expansion. The bottom of the cell, made of copper (Figure 4), displays two holes allowing the transmission of light across the grid of the working electrode. The entire cell is then introduced in the inner chamber of the cryostat before injection of the solution (2 mL). Injection under anaerobic conditions is carried out through the inlet port at the side of the copper block. This OTTLE cell model was shown to be very versatile (IR and UV-Vis-NIR measurements), and robust (no leakage on a timescale of hours). Moreover, it offers the advantage of allowing spectroelectrochemical measurements under inert atmosphere at very low temperature since liquid nitrogen is the coolant. Also, the OTTLE cell is demountable and can be quite easily cleaned. Although this setup displays many advantages, it has the main drawback of only allowing the use of metallic grids, which may be an issue when side reactions, such as proton reduction at a Pt surface, have to be avoided.

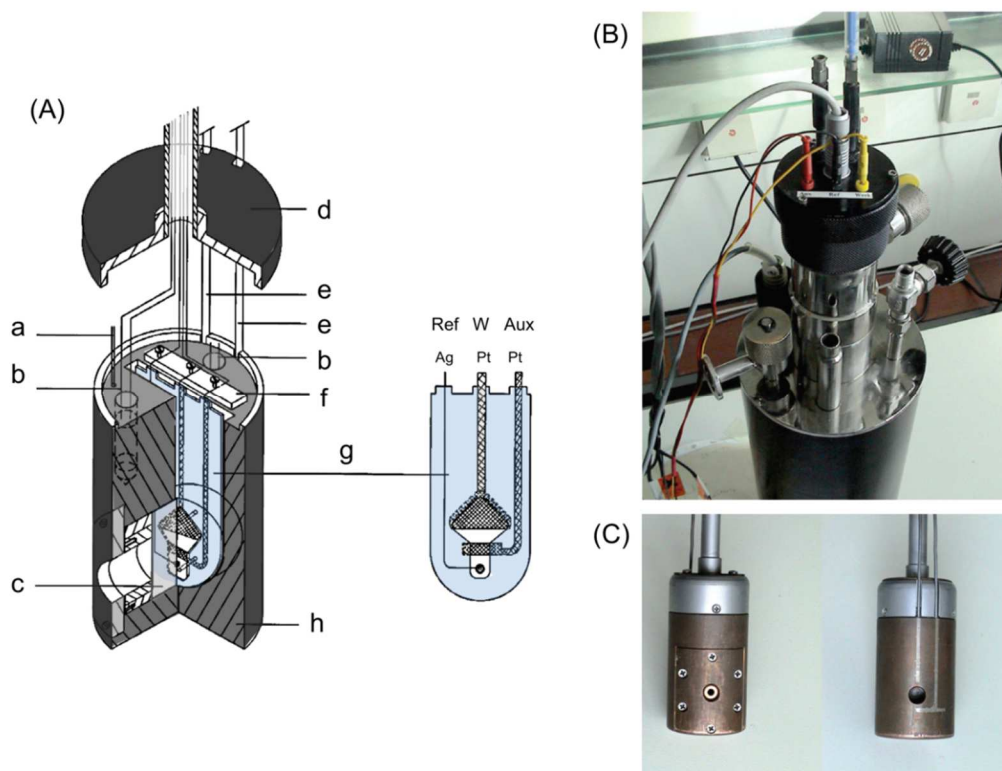


Figure 4. A) Schematic view of the low-temperature UV-Vis and IR spectroelectrochemical set-up developed by Hartl *et al.*: (a) Pt-100 thermocouple, (b) Heaters, (c) CaF₂ windows, (d) Upper cover

plate, (e) Vacuum-tight (soldered) throughputs for the 1/4-inch solution inlet and outlet tubes, (f) Insulating PTFE plate, (g) Polyethylene melt-sealed three-electrode system, (h) Cylindrical copper block. Reprinted with permission from [95], copyright (2003) CCCC. B) Detailed view of the top part of the cryostat with the thin-layer cell positioned in the inner chamber. C) Detailed view of the front and rear sides of the copper body of the inner thin-layer cell, showing the frontal pressure plate with fixation screws and the soldered air-tight thin-layer filling. Reprinted with permission from [95], copyright (2003) CCCC.

1.4.1.2. Low-temperature reflection thin-layer cells.

In parallel to the development of low- T OTTLE cells, several research groups have designed systems based on the reflection of the optical signal on the electrode surface. The low-temperature infrared reflection-absorption spectroscopic (IRRAS) cell designed by Best and co-workers in 1987, and further improved [96], was constituted of two Teflon blocks which were screwed-assembled [97]. The working electrode, a 1-10 mm diameter Pt/Au disc in contact with the central brass rod, was finely brought close to an infrared transmitting window (KBr/quartz) by a micrometer adjustment. The resulting thin layer (1-10 μm) of solution was irradiated by an external source through the front window. The reflected signal was recovered by appropriate collection optics onto the detector. As for OTTLE cells, diffusion of solute in and out of the thin layer was relatively slow because the working and counter electrodes were considered as separated. Cooling of the solution was achieved by passing cold nitrogen through channels machined into the central brass rod. The solution was degassed *in situ* and maintained under an inert atmosphere. Best and co-workers showed that effective electrolysis of species within the thin layer could be achieved in approximately one minute, thus allowing the characterization of transient species at 253 K. This model offers thus the advantage of very fast transformation since the volume of the thin layer is significantly small as compared to the dimensions of the electrode surface. Nevertheless, it should be noted that the control of the temperature within the thin layer is not explicitly detailed in the mentioned articles.

Following the same principle, Kubiak and co-workers designed a reflectance spectroelectrochemical cell which could be used at low temperature [98, 99]. Main differences with Best's model concerned the disposition of the electrodes and the cooling system. As shown in Figure 5, a circular working electrode (WE; Pt, Au, or glassy carbon) is surrounded by concentric rings of Ag and Pt electrodes which play the role of pseudoreference and counter electrodes, respectively. All electrodes face down on a thin Teflon spacer (< 0.5 mm) on top of a CaF_2 window. The volume of the thin-layer chamber is small (several hundreds of μL) and kept under controlled atmosphere with the help of syringes. The temperature of the solution within the cell is decrease by circulating a cooled liquid (low viscosity silicone) through inlet and outlet ports built integrated into the system. Since a pseudo-reference electrode is used, the real redox potential is determined by addition of a well-known redox couple, such as ferrocenium/ferrocene.

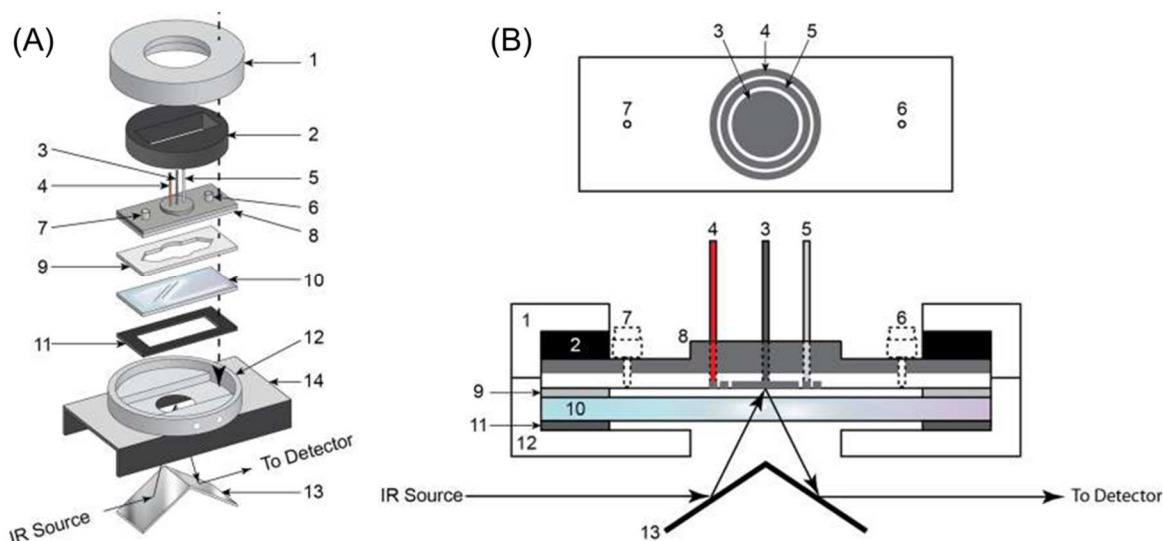


Figure 5. A) Disassembled and B) compact views of the spectroelectrochemical cell proposed by Kubiak and co-workers [98, 99]. (1) Tightening brass cap (threaded inside); (2) brass ring required to tighten the cell; (3) working electrode; (4) auxiliary electrode; (5) pseudo-reference electrode; (6, 7) injection ports; (8) cell body, top part aluminum, lower part Teflon; (9) Teflon spacer; (10) CaF_2 window; (11) rubber gasket; (12) hollow brass cell body with threaded inlet and outlet ports for connection to circulating bath; (13) mirrors; (14) two-mirror reflectance accessory. Reprinted with permission from [99], copyright (2014) American Chemical Society.

Another design of low- T spectroelectrochemical setup base on the combination of fiber optics and a reflective working electrode was reported in 1992 by Salbeck [100]. In his model, the electrochemical cell was a conventional three-electrode system with a Pt disc working electrode (diam. 3 mm), a concentric counter electrode (stainless steel electroplated with nickel and gold) and an AgCl-coated silver wire as the pseudo-reference electrode. The cell vessel consisted of a cylindrical quartz cuvette equipped with an optical window at the bottom. The optical signal carried by a fiber optics bundle was directed towards the surface of the reflective platinum working electrode at the bottom of the cell vessel. The distance between the working electrode and the floor of the cell was finely varied by using a micrometer, hence allowing different diffusion conditions (finite (thin-layer) and semi-infinite). The quartz cell was sealed by a Teflon head and rested in a brass support displaying cooling channels and connections for a cryostat. A similar model was proposed by Gaillard and Levillain in 1995 [12]. The spectroelectrochemical cell, made of Teflon and polyethylene, was designed such that quasi-reference and counter electrodes (2 mm diameter tungsten rods) were placed on each side of the working electrode (5 mm diam. Pt disk). As for Salbeck's model, semi-infinite or thin layer diffusion

conditions were obtained by translating the working electrode by a micrometric screw. A nine fibers bundle was used to guide the light to the cell, and ten fibers collect the reflected light from the cell to the spectrophotometer.

Still in reflectance mode, an *in situ* low- T IR spectroelectrochemical cell was proposed by Shaw, Richter-Addo and co-workers in 2006. This model, initially designed for room-temperature studies [101], could be modified for experiments at low temperatures by jacketing the cell into a dry ice-acetone bath at 195 K [102]. The principle was to adapt a commercial Pt working electrode such that it fits into the end of a mid-IR fiber-optic probe, in place of the usual stainless steel mirror present in the transmission cell. A silver wire coated with silver chloride was used as the reference electrode and a platinum wire served as the auxiliary electrode. Hence, changes of species concentration and nature within the thin layer separating the electrode and the probe could be monitored by reflectance of the optical signal. According to Shaw *et al.*, this system was superior to OTTLE and IRRAS models because the iR drop was significantly smaller due to the small size of the working electrode, allowing monitoring of the composition of the solution by IR spectroscopy at the CV timescale. Moreover, the authors argued that their experimental setup was simple, required little preparation, allowing the use of reflective carbon electrode, and yielded results rapidly.

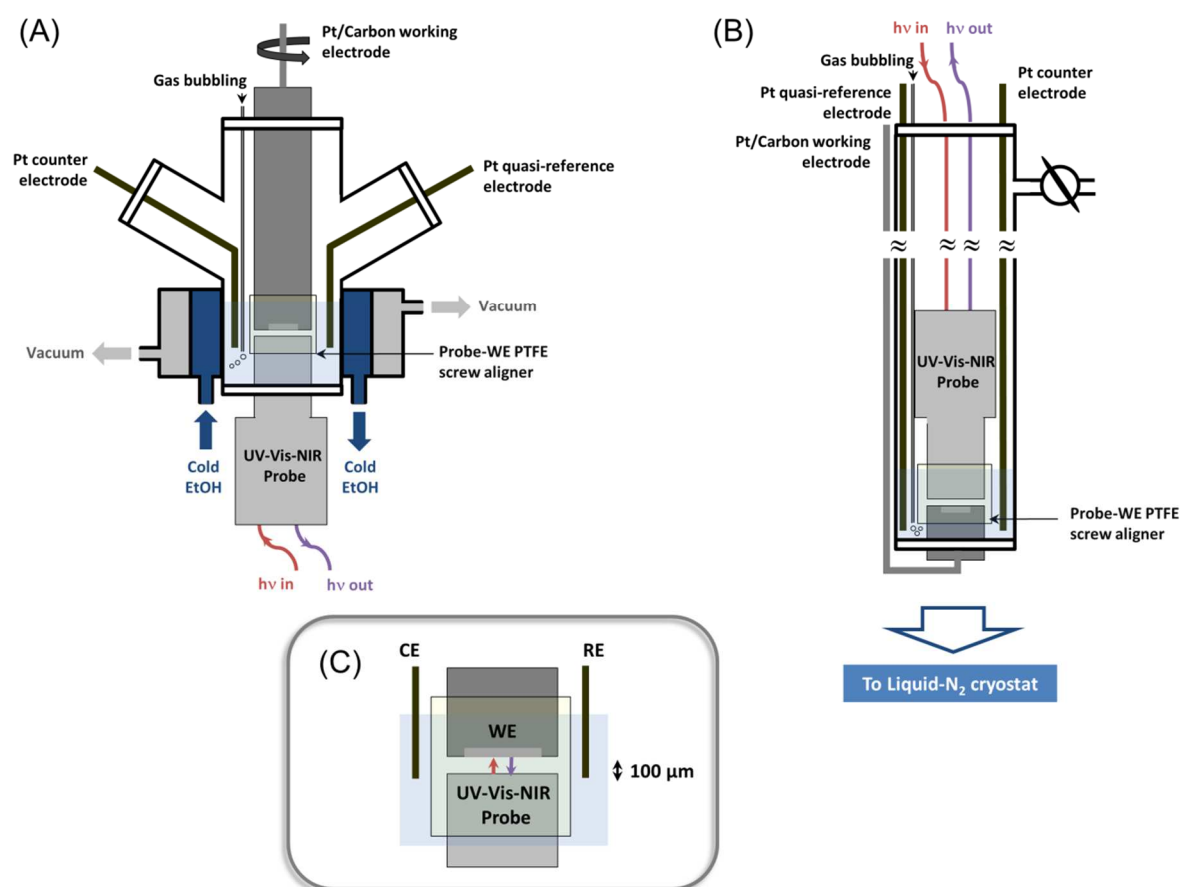


Figure 6. Schematic views of the low- T spectroelectrochemical cells developed by Le Poul and co-workers. A) model with double-jacket cooling; B) model with a Schlenk tube for insertion in a liquid- N_2 cryostat; C) principle of the reflectance measurement at the probe-electrode interface.

This optic-fiber probe concept was more recently re-engineered by Le Poul and co-workers for UV-Vis-NIR measurements at temperatures down to 183 K (Figure 6). In a first model, a classical three-electrode glass cell containing a Pt/GC working electrode disk of 3 mm diameter, a Pt wire counter electrode, a Pt wire pseudo-reference electrode or a Ag/AgNO₃ reference electrode in a separate compartment, was adapted to allow the insertion of a commercial UV-Vis probe by the bottom face. Two overlaying jackets were surrounding the sample space: the first one contained the cold fluid (EtOH) circulating between a cryo-cooler and the cell. The second jacket, under dynamic vacuum, was designed to insulate the cold chamber from outside. This reflectance mode system was used for low-temperature spectroelectrochemical measurements in a glovebox. The second model designed by Le Poul and co-workers was inspired by both Hartl's and Shaw/Richter-Addo set-ups. It consisted of a long (40 cm) Schlenk tube, containing one Pt or glassy carbon disk working electrode at the bottom, as well as two Pt wires (reference and auxiliary electrodes) and one fiber-optic probe on the top. As for the first model, all elements could be disassembled and easily cleaned. For low-temperature measurements, the Schlenk tube was introduced into a liquid-nitrogen cryostat. As for the first model, the optical signal was sent and reflected onto the working electrode and analyzed in a time-resolved manner, thanks to a PTFE screw aligner. All the inside chamber was air-tight, and small volumes of solution (typically 1 mL) were used. Bubbling of specific gas was allowed by a PTFE tube from the top of the cell to the bottom of the solution.

1.4.2. EPR cryo-spectroelectrochemical cells

The design of EPR spectroelectrochemical cells, also coined as SEEPR or SEESR cells (for simultaneous electrochemical-electron spin resonance), was initiated in the 1960s for the room-temperature characterization of EPR-detectable organic radicals. Low- T EPR spectroelectrochemical studies were first achieved in 1976 by Allred and co-workers by using a flat cell surmounted by a solution flask [50]. The quartz cell was constituted of Pt working and quasi-reference electrodes, connected to the top of the assembly, and a Pt counter electrode at the bottom. The solution (20-100 mL) was cooled down to 173 K by circulating cold nitrogen gas into baffles. The cold nitrogen was passed along the flat cell and out a small hole at the bottom. A vacuum jacket surrounding the active area of the ESR cavity was used to prevent condensation of moisture. Another cell design was further proposed by Kadish *et al.* with a column-shaped thin-layer model cell which could be used at ambient and low temperatures [103]. Complete electrolysis of the thin-layer chamber was achieved between

40 to 120 seconds after applying a controlled oxidizing or reducing potential. The cell was placed in a jacketed Dewar, which was mounted in the cavity and was bathed in a stream of chilled N₂ gas.

Alternatively, Bond and co-workers proposed from 1983 various models of EPR spectroelectrochemical cells for room and low-temperatures studies [87, 104-109]. The Figure 7A displays one example of cell reported in 1988 which was used in both stationary and flow-through configurations at variable temperature [108]. The cell was a 4 mm tube made of Pyrex glass. A platinum wire, serving as working electrode, was sealed into the lower end. The nature of the working electrode could be modified by electroplating of gold/silver on the Pt wire, or even introduction of a drop of mercury at the bottom of the cell. The ohmic drop was minimized by positioning the working electrode and the tip of the reference electrode very close to each other [106]. Bond *et al.* demonstrated that the cell, which was easy to manufacture and handle, could be suitable for solvents with low and high dielectric constants.

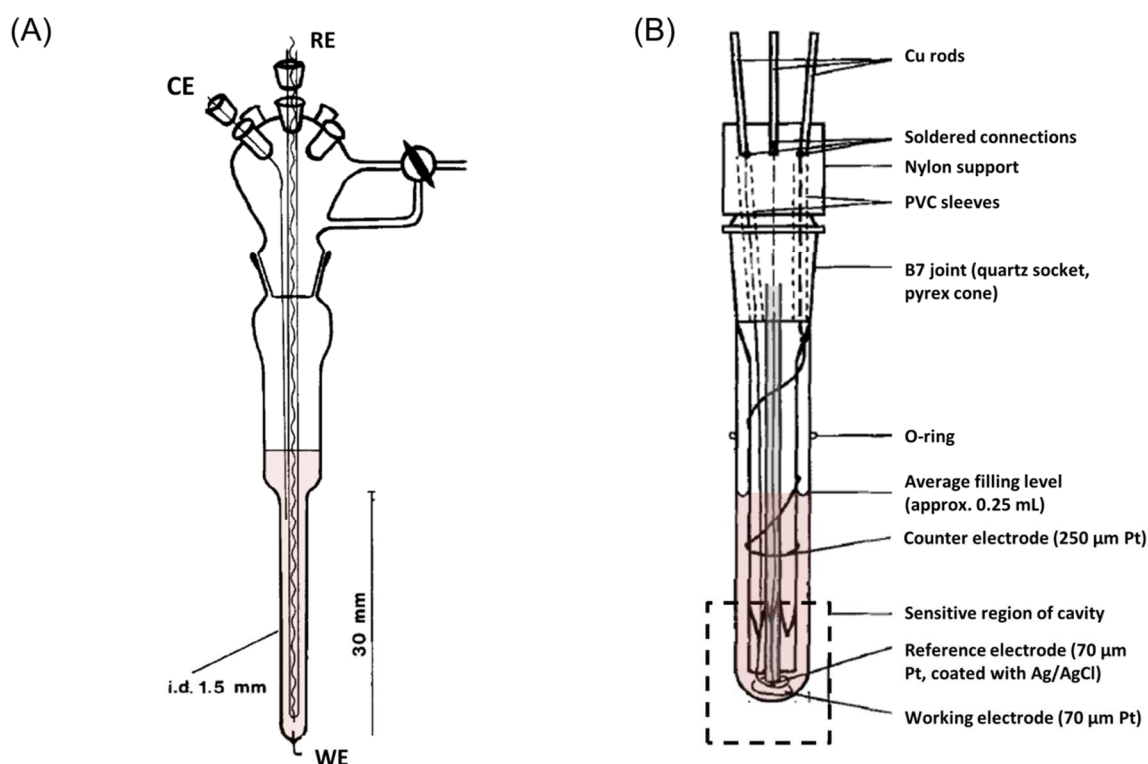


Figure 7. Low-*T* EPR spectroelectrochemical cells developed by Bond and co-workers. A) model developed in 1988. Reprinted with permission from [108], copyright (1988) Elsevier B.V.. B) model developed in 1995. Reprinted with permission from [87], copyright (1995) IOP Publishing.

A small volume (0.2 ml) EPR spectroelectrochemical tubing cell was further developed by the same group in 1995 (Figure 7B). It was specifically designed to allow studies of electrochemically generated highly oxygen and/or moisture sensitive radicals at low temperature with low and high-dielectric constants solvents. The reference electrode, a Pt wire coated with Ag/AgCl, was inserted in a

1 mm diameter pyrex glass tube. The working electrode (Pt wire 70 μm diameter) and the reference electrode assembly were then both inserted in a second pyrex tube for larger diameter (2 mm). With this setup, few seconds were necessary to monitor changes of the EPR response by fast electrolysis (scanning or potential step).

Based on the Allendoerfer works [110], Hartl *et al.* reported in 2001 an air-tight EPR spectroelectrochemical cell equipped with a gold-helical working electrode of large active surface, a Pt helix counter electrode wound on a supporting glass rod and a silver wire pseudo-reference electrode placed in the electrolysis chamber [111]. This design allowed the possibility to undertake spectroelectrochemical measurements at low temperatures in a leak-proof environment. Fast electrolysis (< 30 s) could be achieved thanks to the relative low volume of solution and high area of the working electrode.

Compton *et al.* reported hydrodynamic spectroelectrochemical EPR measurements at low T with coaxial tubular flow cells [112, 113]. The cells consisted of parallel back-to-back inlet and outlet channels, connected at the bottom to form a U-tube configuration. Working and quasi-reference electrodes were positioned in the inlet channel, and two large counter electrodes (Pt and Au) were located in the outlet channel, upstream the edge of the cavity.

It is worth underlining that amongst the different examples of low- T EPR spectroelectrochemical cells which have been above-described, a great majority of the studies have been achieved with liquid solutions, i.e. EPR and electrochemistry were simultaneously undertaken, through stationary or flowing modes. Nevertheless, most of EPR spectroscopic studies of transition metal complexes are usually performed with frozen solutions for the determination of anisotropic values of g and A tensors. In fact, concomitant *in situ* EPR spectroelectrochemical characterization of metal complexes is often not compatible for metal complexes with a well-resolved (anisotropic) EPR signature. The classical approach to overcome this issue is to perform electrolysis of the solution at a temperature just above the freezing point of the medium. Once the electrolysis is completed, the temperature is decreased below the freezing point of the liquid electrolyte such that solid-state EPR measurements can be performed. Although detection is undertaken *in situ*, it cannot be considered strictly as simultaneous.

1.4.3. Multi-spectroelectrochemical cells

The simultaneous combination of multiple spectroscopies with electrochemical methods has emerged in the mid-1990s under the impulsion of Dunsch and co-workers. The “multi-spectroelectrochemistry” concept consists of making concomitant spectroelectrochemical measurements (UV-Vis, EPR, Raman, IR...) within the same cell in a single experiment. Simultaneous application of both EPR and UV-Vis-NIR spectroscopies in a single *in situ* spectroelectrochemical technique at the same working electrode was first demonstrated thanks to the development of an optical EPR cavity [114]. Various organic molecules, redox polymers, as well as composite structures of carbon nanomaterials and polymers were

thus investigated at room temperature by these techniques [115]. However, rare examples of low- T *in situ* EPR/UV-vis-NIR spectroelectrochemical techniques were reported [116, 117]. For example, *in situ* and simultaneous EPR-Vis-NIR characterization of the radical cation generated by electrochemical oxidation (CV) of N,N,N',N' -tetramethyl-1,4-phenyldiamine was reported in 2001 [117]. For these measurements, the spectroelectrochemical setup consisted of an EPR flat cell in which a laminated Pt-mesh working electrode, a silver wire pseudo reference electrode and a Pt wire counter electrode could be inserted. The cell was positioned in a Dewar located inside the EPR optical cavity. The front optical opening of the cavity was adapted for the light guide from the two continuous light sources. UV-vis-NIR spectra were taken using a photodiode array spectrometer on the other side of the source, such that light passed through the Pt mesh. Temperature control of the cavity was operated by using standard setup for EPR systems (chilled N_2 gas).

2. Low-temperature electrochemistry for coordination or organometallic compounds

In the following section, we discuss several examples of low-temperature electrochemical experiments illustrating the great utility of these methods to afford valuable information related to: (i) the determination of the thermodynamics and kinetics of electron transfer reactions, (ii) mechanistic studies of chemical-coupled electron transfer reactions and characterization of the transient species. The second aspect is usually associated to spectroelectrochemical experiments, as treated in section 3.

2.1. Determination of the thermodynamics and kinetics of electron transfer reactions

Table 3 gathers data for some inorganic and organic compounds which have been investigated by low temperature electrochemical techniques for the quantification of redox and diffusion parameters (number of electrons, kinetics and thermodynamics of electron transfer, mass transfer...). As clearly shown in the Table 3, the main technique for low-temperature measurements is cyclic voltammetry. A.c. impedance (EIS) approaches have been used in rare cases, as well as chronoamperometry and chronocoulometry.

Metallocenes have been thoroughly investigated mainly because of their inherent low inner-sphere reorganizational energy upon electron transfer. Van Duyne and Reilley were amongst the first to perform CV experiments with ferrocene in aprotic solvents down to 194 K [5]. They found that the half-wave potential (assumed as E^0) of the Fc^+/Fc redox couple shifted by 0.31 mV K^{-1} . Activation enthalpy for diffusion was also evaluated from chronocoulometric methods. In 1991, Fawcett and co-workers measured the heterogeneous standard rate constant for the electrochemical oxidation of ferrocene in three alcohols-based solvents at a Pt electrode from 190 K to 295 K by using $LiClO_4$ as supporting electrolyte [72]. The resulting activation parameters were compared to theoretical data obtained from Marcus theory using the mean spherical model (MSA) for ionic solvation. Murray *et al.*

studied the electron transfer for decamethylferrocene (DMeFc) at a gold microband, as well as a poly(osmium) complex deposited on Pt, in the cryo-mixture of solvents EtCl/PrCN [31]. Remarkably, they showed that the thinner polymer film was better discernible at ultra-low temperature (103 K) than the thicker one. They interpreted this phenomenon as resulting from an increasing barrier to ion diffusion accentuated as the amorphous polymer matrix becomes increasingly rigid at lower temperatures. Ferrocene and derivatives were also used for the study of superconductivity onset with HTSCs. Since several oxocuprates were able to attain their superconducting state above 100 K, several studies have been performed in order to investigate charge transfer at HTSC electrode / liquid electrolyte interface, using metallocenes as redox probe (diffusing or attached) [16, 42, 44-46, 118]. The group of Murray was the first in 1988 to report CV at a HTSC electrode at low temperature (183 K) in dichloromethane using DMeFc as redox species [118]. In 1992, Rosseinsky and co-workers described cyclic voltammetry studies of diffusing ferrocene at a HTSC electrode in its superconducting state ($T_c = 105$ K), by using a mixture of chloroethane and tetrahydrofuran. Nevertheless, for both of these examples, no data was extracted from the CVs. In 1995, Murray and co-workers coated HTSC electrode surfaces with a thin layer of Ag and Fc-terminated self-assembled monolayers (SAMs) [45]. Suitable length of the alkane chain of the SAM allowed estimation of electron transfer rate from the electrode to the Fc moiety, by using chronoamperometry. Further later, Rosseinsky *et al.* carried out EIS measurements with HTSC electrodes and DMeFc from 111 K to 120 K (Figure 8A). They observed a dip in the charge transfer resistance value at T_c , consistent with the transfer of Cooper electron pairs from the superconductor to the metallocene, as observed with solid electrolytes [42]. The same group performed voltammetric analysis of HTSC electrodes modified with either SAMs [44] or polypyrrole [46] terminated by Fc moieties (Figure 8B). Arrhenius plots of the heterogeneous rate constant displayed a modest effect of superconductivity for both systems, which were ascribed to the difficulty for the chain/polymer to accommodate for the transfer of paired electrons.

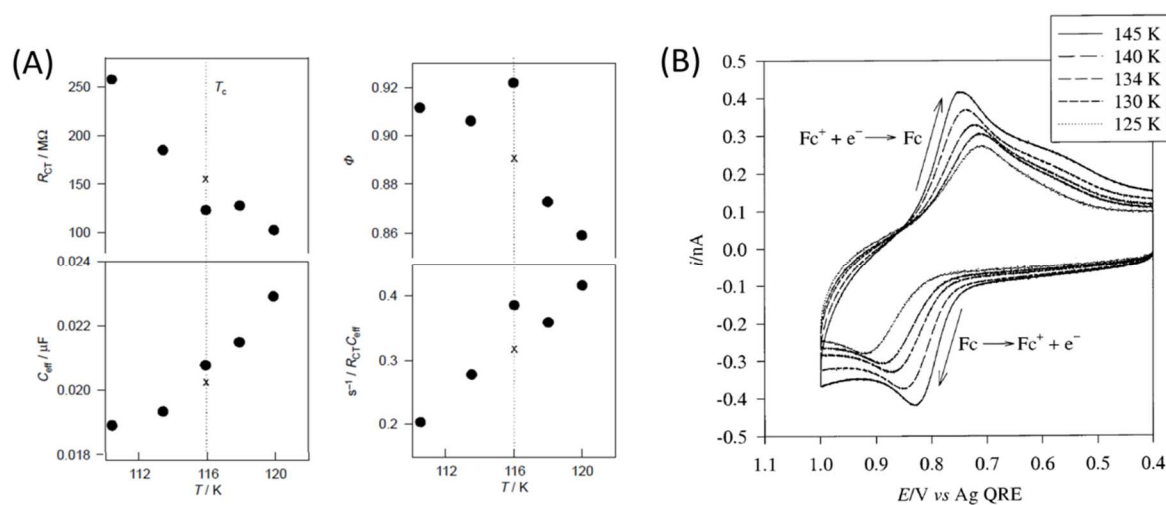


Figure 8. A) Charge-transfer resistance, effective double-layer capacitance, phase parameter and (inverse) effective time-constant observed for DMFc/HTSC at the electrolyte/electrode interface. Reprinted with permission from [42], copyright (1998) Royal Society of Chemistry. B) Temperature dependence of cyclic voltammetry of $\text{Cp}_2\text{FeCO}_2\text{-(CH}_2)_8\text{SH/Ag/Hg}$ -based HTSC in 16:7:1 EtCl/THF/2-MeTHF, containing 0.2 M LiBF_4 ; potential sweep rate 0.005 V s^{-1} . Reprinted with permission from [44], copyright (2003) American Chemical Society.

Besides ferrocene derivatives, a few number of transition metal complexes have also been the subject of studies by low temperature electrochemistry for the determination of thermodynamic and kinetic parameters. For instance, Savéant and co-workers determined the reaction entropy associated to the ET for a series of Fe-porphyrins from plots of formal potential against T (varying linearly from 0 to -0.7 mV/K for $253 \text{ K} < T < 288 \text{ K}$) [34]. They concluded that that entropy factors play a crucial role in the modulation of the reactivity by the molecular superstructures. Copper complexes modeling active sites of oxidases and oxygenases have also recently drawn more attention in terms of low-temperature electrochemistry. In particular, standard potential values of transient copper-oxygen species which are believed to perform hydrogen atom abstraction of strong C-H bonds have been obtained from cyclic voltammetry [119-122].

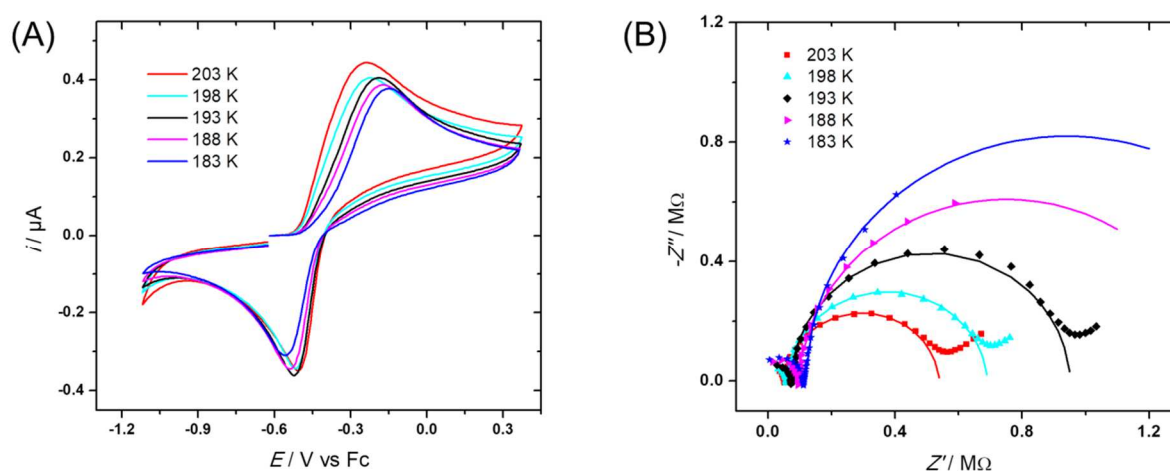


Figure 9. A) CVs ($\nu=0.1 \text{ V s}^{-1}$) and B) complex-plane plots of a dicopper(II)peroxo complex (1 mM) in $0.05 \text{ M NBu}_4\text{ClO}_4/\text{CH}_2\text{Cl}_2$ (Pt WE) for $183 \text{ K} < T < 203 \text{ K}$. Reprinted with permission from [121], copyright (2017) John Wiley and Sons.

Recent works by Le Poul and co-workers have shown that low temperature EIS ($183 \text{ K} < T < 203 \text{ K}$) could also be of interest for the determination of electron transfer kinetics for the heterogeneous electron transfer of dicopper-superoxo/peroxo species (Figure 9) [121]. The reorganizational energy for the process was calculated from Arrhenius plots and was in good agreement with theoretical results. Alternatively, Peters *et al.* studies the ET reaction of iron complexes which can possibly

catalyze ammonia production. Cyclic voltammetry studies at 195 K in a 50 mM NaBAR^F/ THF electrolyte in presence of acid was performed in order to stabilize the transient species [123]. CV analysis provided a value for the standard potential of the protonated complexes; hence, an estimate of the homolytic N–H bond enthalpies could be calculated with the help of acidity titrations.

Table 3. Selected examples of low-temperature studies of coordination and organometallic compounds for the determination of electron transfer thermodynamics and kinetics, as well as diffusion coefficient (in chronological order).

Compound	T_{low}/K	Technique	Aim	Ref.
Fc	194	CV, CC	Cryo-solvents, iR drop, ET kinetics	[5]
[Fe(X-Sal) ₂ trien]	220	Polar.	ET thermodynamics	[23]
Cobaltocenium	223	CV	ET kinetics, thermodynamics, with microelectrodes	[27]
Fc	193	CV	ET kinetics	[72]
DMeFc, poly-[Os(bpy) ₂ (vpy) ₂] ²⁺	98	CV, LSV, CA	Cryo-solvents, diffusion coeff.	[31]
Fe-porphyrins	253	CV	ET kinetics, thermodynamics,	[34]
Fc (as SAMs)	115	CV	ET kinetics	[14]
Fc	99.5	CV	ET kinetics	[17]
DMeFc	130	CV	ET kinetics, diffusion coeff.	[15]
Fc (as SAMs)	150	CV	ET kinetics	[124]
Fc (as SAMs)	140	CV	ET kinetics	[29]
Fc (as SAMs on HTSCs)	105	CV	ET kinetics	[45]
[Fe(CN) ₆]K ₄	170	CV	ET thermodynamics	[58]
DMeFc with HTSCs	102	EIS	ET kinetics	[42]
Fc (as SAMs on HTSC)	125	CV	ET kinetics	[44]
Poly(pyr-Fc) on HTSC	110	CV	ET kinetics	[46]
[Cu(MePY2) ^R (O ₂)] ²⁺	195	CV	ET thermodynamics	[125]
DMeFc	120	CA, CA, EIS	ET kinetics	[20]
Fc	173	CV	Diffusion coeff.	[126]
FeCp ₂ , RhL ₂ , RhL ₂ -FeCp ₂	253	CV	ET thermodynamics	[127]
Fc	188		ET kinetics	[128]
Fc, Cc	258	ACV	ET kinetics	[129]
Cytochrome c	260	CV	ET for biological compounds in low-T conditions	[21]
[Cu(tmpa)] ₂ -(μ-OH)	243	CV	ET thermodynamics	[119]
Pyrazolate-based μ-1,2-peroxo dicopper(II)	273	CV	ET thermodynamics	[120]
Phenoxy- μ-1,2-peroxo dicopper(II)	183	CV, EIS	ET kinetics and thermodynamics	[121]
[P ₃ ^{Si} Fe–N=NMe]	195	CV	ET thermodynamics	[123]
[Cu(L)(OH)] (L=bis-diiso)	266	CV	ET thermodynamics	[122]

propylphenyl)carboximido
pyridine)

Abbreviations: CV (cyclic voltammetry), EIS (electrochemical impedance spectroscopy), Polar. (polarography), ACV (a.c. voltammetry), CC (chronocoulometry), LSV (linear sweep voltammetry), DPV (differential pulse voltammetry), CA (chronoamperometry).

2.2 Mechanistic studies of chemical-coupled electron transfer reactions

Low-temperature electrochemical techniques have also (and mainly) been of interest for the understanding of coupled chemical-electrode reactions and the characterization of transient species. The Table 4 gathers several examples of low- T studies including inorganic and organic compounds. Clearly, cyclic voltammetry appears as the most popular and adequate electrochemical technique for such purposes. One main reason is that CV offers a direct visualization of the transient species through the reversible/irreversible shape of the curve. Moreover, determination of the thermodynamic and kinetic constants associated to the coupled chemical reactions for EC, CE, ECE and related processes can be easily accessed by numerical methods, analytical expressions and/or voltammetric simulations. Figure 10 provides an example of CV study for an ECE process by Kadish *et al.* on a rhodium complex [75]. The mono-Rh(III) complex displayed an irreversible reduction peak at room temperature, further followed by a reversible system in reduction. When T was decreased down to 195 K, reversibility was obtained on the first system and a new reversible peak was detected in reduction. The ECE mechanism proposed by the authors is depicted in Figure 10. The first monoelectronic reduction at $E_{1/2}(1)$ is metal-centered, leading to the generation of $[\text{Rh}^{\text{II}}\text{L}_2]^0$. Fast ligand unbinding occurs at room temperature leading to dimerization and formation of $[\text{Rh}^{\text{II}}\text{L}]_2^0$. This species is then reduced at $E_{1/2}(2)$. Hence, low temperature provided the opportunity to decrease the dimerization process and allowing the characterization of the $[\text{Rh}^{\text{II}}\text{L}_2]^0$ species.

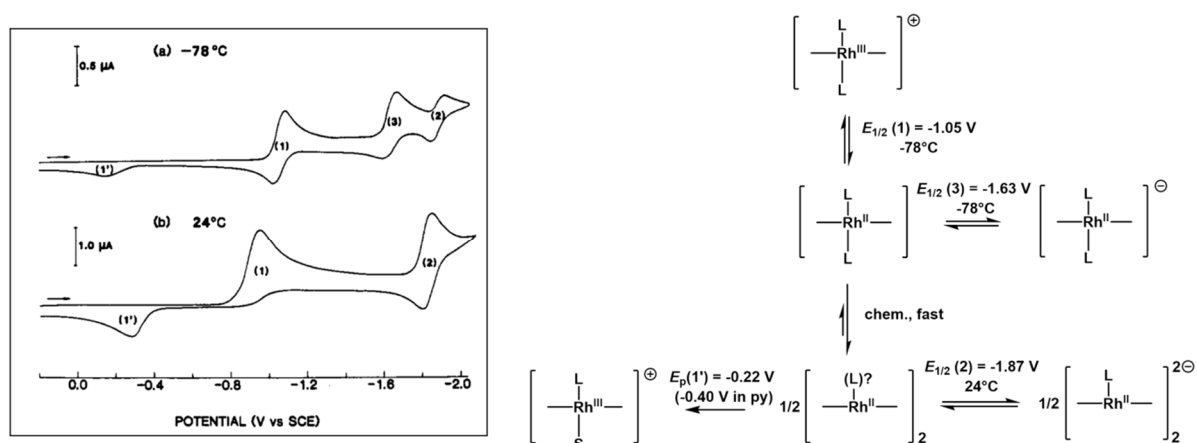


Figure 10. CVs of $[(\text{TPP})\text{Rh}(\text{L})_2]^+\text{Cl}^-$ in 0.2 M $\text{NBu}_4\text{ClO}_4/\text{THF}$ at (a) 195 K and (b) 297 K ($\nu = 0.2 \text{ V s}^{-1}$). Reprinted with permission from [75], copyright (1985) American Chemical Society.

In 2013, Storr and co-workers reported low-temperature voltammetric studies (230 K) of Ni-salen complexes (Figure 11) [130]. Their purpose was to sufficiently stabilize the radical and bis-radical species generated by electrochemical oxidation within the timescale of experiment such that they could evaluate the degree of interaction between the phenolate moieties. The mono-metallic complex was shown to undergo two reversible redox processes assigned to ligand-based oxidation processes, forming the mono- and bis-phenoxy radical species. The degree of electronic delocalization of the phenoxy radical was determined from the comproportionation constant, K_c , calculated from the difference between the first and second oxidation potentials. A high value of K_c , was obtained, pointing out significant coupling between the redox-active phenolates in its mono-oxidized state. The dinuclear complex exhibited a different behavior since the two first mono-electronic processes were occurring at very close formal potentials, indicating that the coupling between the two salen units was limited. However, it is worth to mention that K_c cannot be considered a good and robust parameter to evaluate electronic coupling as it has been thoroughly discussed in the literature [131-133].

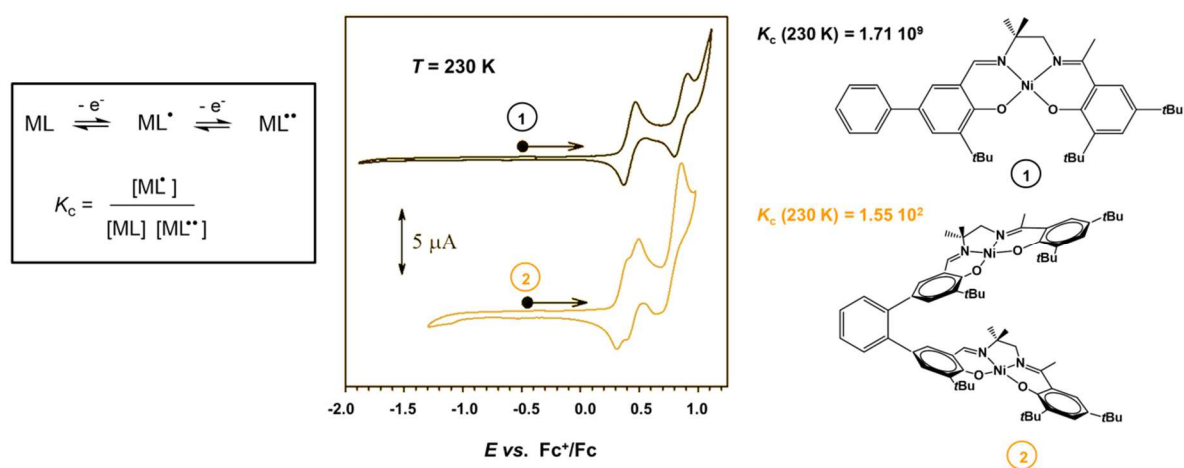


Figure 11. CVs ($v = 0.1 \text{ V s}^{-1}$, $T = 230 \text{ K}$) of mono and bis-Nickel(II) salen complexes in $0.1 \text{ M NBu}_4\text{ClO}_4/\text{CH}_2\text{Cl}_2$. The electrochemical data was used for the calculation of the comproportionation constant K_c for each complex. Reprinted with permission from [130], copyright (2013) John Wiley and Sons.

Electrochemical characterization of transient species, such as metal-oxo, hydroperoxo and peroxy adducts, was also performed by CV at low-temperature [92, 134-136]. In 2015, Anxolabéhère-Mallart and co-workers reported the study of metastable Fe-oxo and Fe-hydroperoxo species generated by reaction of a Fe(II)-TPEN complex with adequate oxidants (*m*-CPBA and H_2O_2 , respectively) [134]. The iron-oxygen adducts were concomitantly characterized by UV-Vis spectroscopy at low temperature. On one hand, CV at $T = 273 \text{ K}$ of the Fe(IV)=O complex showed an irreversible two-electron reduction resulting from an ECE process which involved the formation of a Fe(III)-hydroxo species (Figure 12A). On the other hand, the hydroperoxo Fe(III)(OOH) adduct generated by excess of

H₂O₂ displayed an irreversible one-electron reduction wave at $T = 228$ K (Figure 12B). The authors suggested from CV simulations that the reductive process did not induce the O-O bond cleavage. Further addition of base led to the formation of the iron(III) peroxy adduct and its characterization by CV at 228 K.

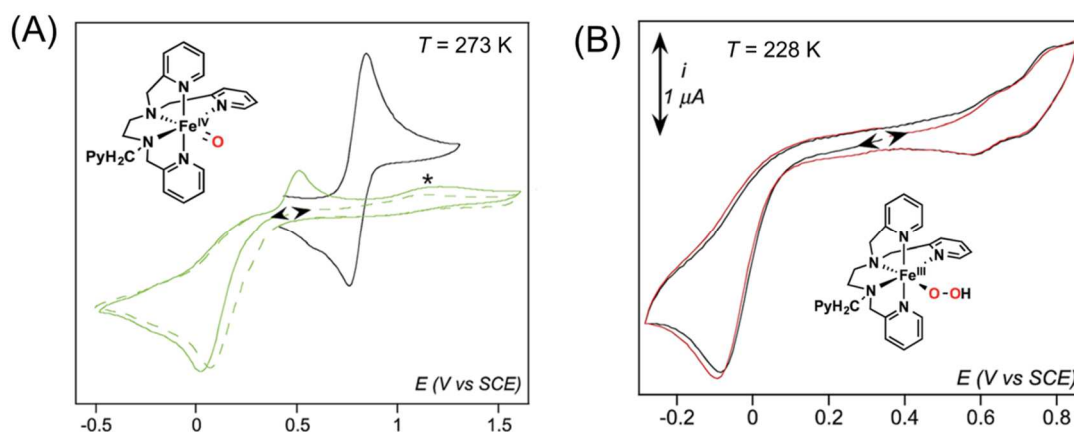


Figure 12. A) CVs ($\nu = 0.1$ V s⁻¹, $T = 273$ K) of [Fe^{II}(TPEN)]²⁺ (black) and [Fe^{IV}(TPEN)(O)]⁺ (green) in 0.1 M NBu₄PF₆/CH₃CN. B) CVs ($\nu = 0.1$ V s⁻¹, $T = 273$ K) of [Fe^{IV}(TPEN)(OOH)]²⁺ in 0.1 M NBu₄PF₆/CH₃CN. Reprinted with permission from [134], copyright (2015) Royal Society of Chemistry.

Table 4. Selected examples of low-temperature studies of coordination and organometallic compounds for the characterization of transient species and the mechanistic studies of chemical-coupled electron transfer reactions (in chronological order).

Compound	T_{low}/K	Technique	Aim	Ref.
NiCp ₂	233	CV	Characterization of Ni(IV) species	[10]
[M(CO) ₂ X] ₂ (M = Mo and W; X = Br and I)	198	ACV, CV	Characterization of Cr(II) species	[64]
[M(Cyclam)] [BF ₄] ₂ M=Hg, Ni, Cu, Ag, Zn	195	CV	Characterization of M(III) species	[50]
Rh-Porphyrins	195	CV	Kinetics of Rh(II) dimerization	[75]
Fe-Porphyrins	183	CV	Characterization of high-spin six-coordinate Fe porphyrin	[68]
Cr-Porphyrins	183	CV	Characterization of six-coordinate Cr porphyrin	[70]
[Co ₄ (CO) ₁₀ (PPh) ₂]	203	CV	Ligand exchange for electrocatalysis	[137]
(Benzene)tricarbonylchromium	183	CV, CC	Characterization of Cr(IV)	[33]

m			species. Effect of counterion	
[Ru(bpy)(5,5'-COOEtbpy)] ²⁺	223	CV	Characterization of transient reduction products	[138]
[Fe(CO) ₂ (Cp)] ₂	195	CV, LSV, CA	Kinetics of radical dimerization	[73]
(Bu ₄ N)Re ₂ Cl ₉	220	CV	Characterization of Re ₂ Cl ₉ ⁴⁻ transient species.	[69]
(Mesitylene)W(CO) ₃	228	CV	Thermodynamics and kinetics of ligand exchange	[66]
(NBu ₄) ₂ [Re ₂ (NCS) ₈]	215	CV	Characterization of [Re ₂ (NCS) ₈] ³⁻ and [Re ₂ (NCS) ₈] ¹⁻	[139]
[M(mnt) ₃] ²⁻ (M)V, Mo, Re)	213	CV	Characterization of transient species	[96]
[Ru ₁₀ (μ-H)(μ ₆ -C)(CO) ₂₄]	213	CV	Characterization of transient Ru species	[140]
[TcNX ₄] ⁻ (X=Cl, Br)	230	CV	Characterization of transient Tc species	[141]
[TcOX ₄] ⁻ (X=Cl, Br)				
[Cr(CO) ₃ (h ₆ -C ₁₆ H ₁₆)]	213	CV	Characterization of transient Cr species	[142]
[RhCl(CO)(iPr ₂ Ph-bian)]	218	CV	Reversibility of redox process in coordinating solvent	[95]
[Ir(tropp ^{Ph}) ₂](PF ₆)	233	CV	Characterization of transient species	[143]
Alkylcobalamins	193	CA	Kinetics of reductive cleavage of the Co-C bond	[78]
Mn-NO porphyrin	195	CV	Characterization of transient Mn-NO species	[102]
Ni-terpyridine	243	CV	Mechanism of ligand exchange	[36]
RuCp ₂	233	CV	Thermodynamics and kinetics of dimerization	[37]
[(η ⁶ -C ₆ R ₆)M(CO) ₃] ⁺ (R=Me, Et; M=Mn, Re)	227	CV	Mechanistic studies of dimerization	[144]
Fe(IV)=O porphyrin	213	CV, DPV	Characterization of π-cation radical Fe(IV)=o species	[92]
Bi-metallic Ni-salen complexes	230	CV	Characterization of phenoxy radical species	[130]
Bis(ferrocenyl)dipnictenes	195	CV, DPV	Characterization of transient species	[53]
[Re(imH)(CO) ₃ (phen)] ⁺	233	CV	C-C bond making processes	[145]
[Re(imCH ₃)(CO) ₃ (phen)] ⁺				
[ReCp(CO) ₂ L] ⁺ (L=PPh ₃ , η ² -2-C ₂ Me ₂ H ₂ , η-C ₂ Ph ₂)	253	CV	Mechanistic studies of dimerization	[146]

[Ni(salen)py ₂] ²⁺	223	CV	Characterization of phenoxy radical	[147]
[Ni(1,2-salcn)py ₂] ²⁺				
Os ₂ Cp ₂ (CO) ₄	243	CV	Characterization of radical cation species.	[82]
Os ₂ Cp* ₂ (μ-CO) ₂ (CO) ₂				
[Mo(CO) ₂ (η ³ -allyl)(α-diimine)(NCS)]	183	CV	Mechanistic studies of dimerization	[148]
[Os(CO)(bpy)Cl ₃]	213	CV	Mechanistic studies of dimerization	[149]
[Ni(Salen ^{CF3})]	233	CV	Characterization of radical species	[150]
[Cu(Salen ^{CF3})]				
[Fe(TPEN)] ²⁺	228	CV	Characterization of Fe=O species	[134]
[P ₃ ^B Fe][BArF ₄]	228	CV	Characterization of Fe-N ₂ species in absence /presence of acid.	[151]
[Cu(calix[6]amidotren)] ²⁺	213	CV	Characterization of Cu(I) species in absence /presence of O ₂ .	[135]
[Mo(CO) ₂ (η ³ -allyl)(x,x'-dmbipy)(NCS)]	195	CV	Mechanistic studies of dimerization	[152]
[Cu ₂ (μ-OH)(μ-OPh)(BPA)(BA)] ⁺	213	CV	Characterization of transient mixed-valent species	[136]
1,1'-diphenyl-2-cymantrenylbutene	253	CV	Mechanistic studies of redox-driven ligand substitution	[83]
[Re(3,3'-DHBPY)(CO) ₃ Cl]	195	CV	Mechanistic studies of H-bonding	[153]

Abbreviations: CV (cyclic voltammetry), EIS (electrochemical impedance spectroscopy), Polar. (polarography), ACV (a.c. voltammetry), CC (chronocoulometry), LSV (linear sweep voltammetry), DPV (differential pulse voltammetry), CA (chronoamperometry).

3. Low-temperature spectroelectrochemistry for coordination or organometallic compounds

As it was discussed in Section 2, cryo-electrochemistry offers the unique possibility of decreasing the rate of chemical reactions coupled to heterogeneous electron transfer processes. Therefore, the electrochemical properties of redox couples involving one unstable oxidation state or short-lived intermediates can be evaluated with this method. While ultrafast electrochemical techniques can serve the same purpose, these methods are hardly coupled with spectroscopy to provide additional information on the electronics and structure of the transient species. In contrast, the combination of cryo-electrochemistry and spectroscopic techniques is much simpler, opening the door to a new method called cryo-spectroelectrochemistry which can yield valuable information on the nature and main electronic and structural characteristics of unstable species at room temperature.

Furthermore, many temperature-sensitive compounds involved in biological, catalytic and energy-conversion processes cannot be studied by ultrafast electrochemical techniques at room temperature. For example, Cu/O₂ coordination complexes which are bioinorganic models of key intermediates in reactions catalyzed by Cu-containing enzymes are traditionally prepared by reacting a starting Cu(I) complex with dioxygen at very low temperatures (153 – 193 K) in organic solvents such as CH₂Cl₂, CH₃CH₂CN or 2-MeTHF. The same compounds usually cannot be obtained at room or moderate low temperatures since decomposition of Cu/O₂ complexes occurs under those conditions. Thus, cryo-spectroelectrochemistry enables both the evaluation of the redox properties and the spectroscopic study of the varied oxidation states in this kind of compounds.

The following section provides several examples of low-temperature spectroelectrochemistry for the characterization of transient species. Table 5 gathers other examples taken from literature in chronological order, for mainly three techniques: UV-Vis-NIR, IR and EPR.

Great effort was made by Bond and co-workers in the 1980s to develop suitable cryo-electrochemical cells for *in situ* EPR spectroscopy. In 1986, this group designed a new cell allowing controlled potential electrolysis, voltammetric and electron spin resonance techniques in small volumes of high-resistant electrolytes such as dichloromethane. As a first example, they studied the *fac-mer* isomerization reaction for [Cr(CO)₃(P(R)₃)₃] complexes (R=Me, OMe) upon electron transfer at room and low temperature ($T = 200$ K). In particular, they could stabilize the unstable *fac*-[Cr(CO)₃(P(OMe)₃)₃]⁺ complex at 200 K and showed that it was EPR-silent (Figure 13) [106]. When the temperature was raised, the *fac*-oxidized complex was transformed into its *mer*-stereoisomer which is EPR-responsive. Analysis of the CV data as well as EPR led to the determination of the rate constant of the isomerization reaction of the oxidized complexes.

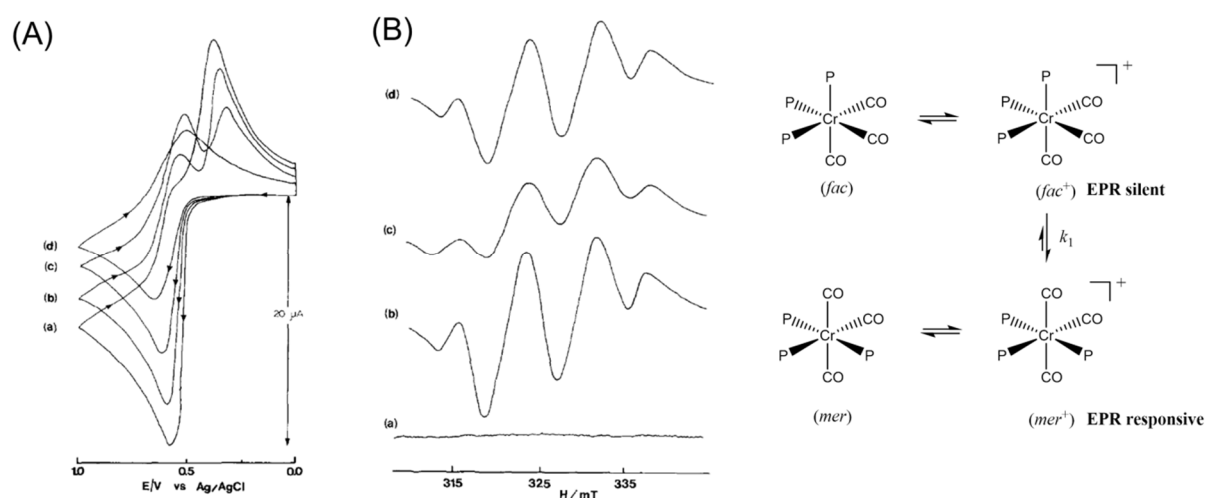


Figure 13. A) CVs of *fac*-[Cr(CO)₃(P(OMe)₃)₃] at a Pt electrode ($v = 0.2$ V s⁻¹) in 0.1 M NBu₄ClO₄/CH₂Cl₂ at a) $T = 279$ K, b) $T = 260$ K, c) $T = 240$ K, and d) $T = 200$ K. B) EPR spectra of in situ generated oxidized species of *fac*-[Cr(CO)₃(P(OMe)₃)₃] at a) $T = 200$ K, b) $T = 240$ K, c) $T = 279$

K, and d) temperature returned to 200 K from 279 K. Right: schematic representation of the *fac-mer* isomerization process upon oxidation of the *fac* species. Reprinted with permission from [106], copyright (1986) Elsevier B. V..

In 1994, Hartl and co-workers reported a versatile cryostated OTTLE cell for UV-Vis and IR spectroelectrochemical measurements at variable temperature [93]. Their novel cell was used for the study of five sensitive compounds from 295 to 173 K under anaerobic conditions. In particular, the electrochemical reduction of ruthenium complexes bearing iPr-DAB ligands (iPr-DAB = N,N'-diisopropyl-1,4-diaza-1,3-butadiene) was investigated by *in situ* IR spectroelectrochemistry (Figure 14). The transient $[\text{Ru}(\text{Me})(\text{CO})_2(\text{iPr-DAB})]^\bullet$ radical species electrogenerated by reduction of the parent complex $[\text{RuI}(\text{Me})(\text{CO})_2(\text{iPr-DAB})]$ was shown to dimerize at ambient temperature in THF, leading to $[\text{Ru}(\text{Me})(\text{CO})_2(\text{iPr-DAB})]_2$. Noteworthy, the dimerization reaction was inhibited by performing the experiment in butyronitrile at 183 K, yielding the stabilized $[\text{Ru}(\text{PrCN})(\text{Me})(\text{CO})_2(\text{iPr-DAB})]^\bullet$ radical species. The discrimination between the dimer and the latter radical complex was obtained from analysis of the IR spectra at different temperatures, supported by UV-Vis spectroscopy.

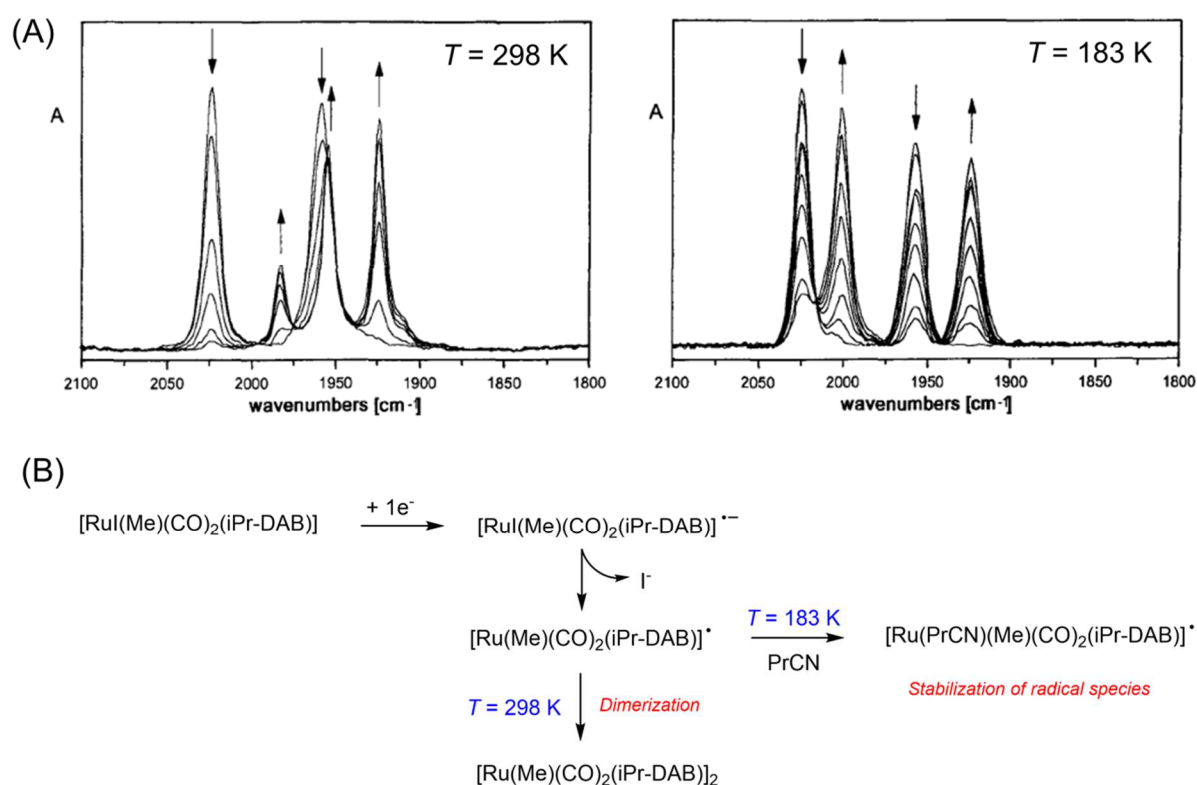


Figure 14. A) Room-temperature (left, $T = 298 \text{ K}$ in $0.1 \text{ M NBu}_4\text{PF}_6/\text{THF}$), and low-temperature (right, $T = 183 \text{ K}$ in $0.1 \text{ M NBu}_4\text{PF}_6/\text{PrCN}$) IR spectroelectrochemistry of the reduction of $[\text{RuI}(\text{Me})(\text{CO})_2(\text{iPr-DAB})]$; B) Proposed mechanisms for the two different temperatures. Reprinted with permission from [93], copyright (1994) Sage Publishing.

In 2011, Fujii and co-workers used low-temperature UV-Vis spectroelectrochemistry for the characterization of transient species resulting from the oxidation of a series of Fe(IV)-oxo porphyrins complexes [92]. Voltammetric studies at $-60\text{ }^{\circ}\text{C}$ revealed that the iron-oxo complexes could be oxidized successively according to two one-electron processes in dichloromethane. For example, the $[\text{Fe}^{\text{IV}}(\text{TPP})(\text{O})]$ complex shown in Figure 15, displayed two reversible systems at 0.1 V s^{-1} at 213 K . Spectroscopic monitoring of the first oxidation at a gold mesh working electrode by *in situ* measurement using an OTTLE cell demonstrated the full transformation of the parent complex ($\lambda_{\text{max}} = 545\text{ nm}$) into $[\text{Fe}^{\text{IV}}(\text{TPP}^{\bullet+})(\text{O})]^+$ which displayed an absorption band at $\lambda_{\text{max}} = 660\text{ nm}$. Oxidation of the $[\text{Fe}^{\text{IV}}(\text{TPP}^{\bullet+})(\text{O})]^+$ radical cation resulted in the formation of an unstable compound at the timescale of the experiment, as shown by the fast evolution of the UV-Vis spectra. Unfortunately, the chemical evolution of the doubly-oxidized species could not be unraveled.

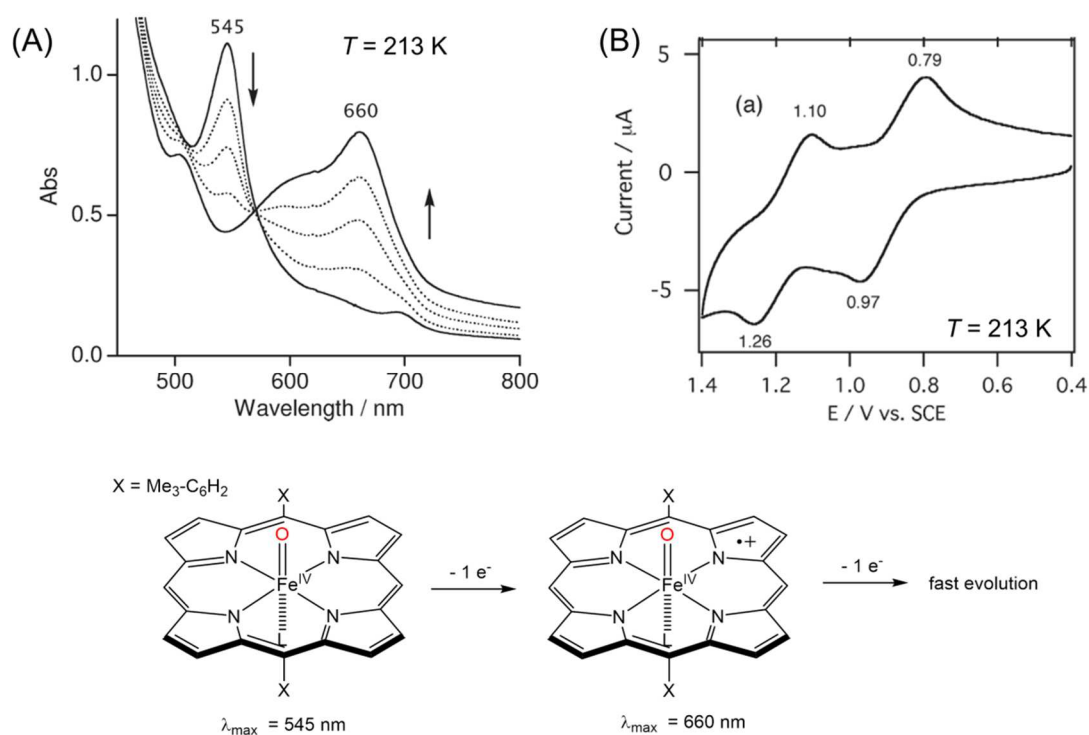


Figure 15. A) UV-Vis spectroelectrochemistry monitoring of the mono-oxidation of the $[\text{Fe}^{\text{IV}}(\text{TPP})(\text{O})]$ complex at 1.10 V vs. SCE in $0.1\text{ M NBu}_4\text{ClO}_4/\text{CH}_2\text{Cl}_2$ at $T = 213\text{ K}$; B) CV of the $[\text{Fe}^{\text{IV}}(\text{TPP})(\text{O})]$ complex at a glassy carbon electrode in $0.1\text{ M NBu}_4\text{ClO}_4/\text{CH}_2\text{Cl}_2$ at $T = 213\text{ K}$. Reprinted with permission from [92], copyright (2011) American Chemical Society.

In 2017, Reinaud and co-workers reported the synthesis and characterization of a Cu(II)-calix[6]arene complex bearing a tris(tren-amide) cap on the small rim of the calixarene ligand, as a model of copper monooxygenases [135]. Electrochemical and spectroscopic studies revealed that two different Cu(I) complexes could be generated by electrochemical reduction of the Cu(II) species. Indeed, at short time

scale (seconds), the Cu(I) complex was shown to react with dioxygen, whereas at long-time scale (minutes), it evolved toward a new Cu(I) species which was insensitive to O₂. In order to probe the transient Cu(II)-superoxo species resulting from the reaction with dioxygen, low-temperature UV-Vis spectroelectrochemistry was carried out by starting from the Cu(II) complex, such that the O₂-reactive Cu(I) could be generated *in situ* according to an EC mechanism, and stabilized. The Figure 16 displays the time-resolved UV-Vis monitoring of the reduction of the Cu(II)-calix[6]trenamide in acetone at 213 K. The appearance of two characteristic bands at $\lambda_{\text{max}} = 400$ nm and 592 nm clearly demonstrated the formation of the Cu(II)-superoxo complex. Importantly, it also indicated that the generated superoxo is not reduced at the potential applied for the reduction of the Cu(II) ($E_{\text{app}} = -0.9$ V vs. Fc⁺/Fc), hence being a rather poor oxidant.

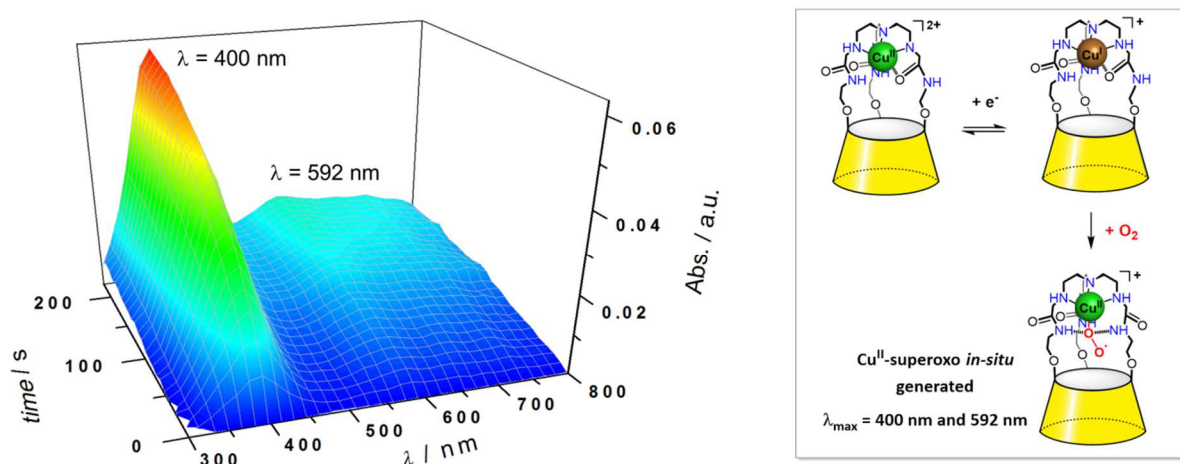


Figure 16. 3D UV-Vis spectroscopic monitoring of the electrochemical mono-reduction of the monocopper calix[6]trenamide complex in 0.1 M NBu₄PF₆/acetone at $T = 213$ K under thin-layer conditions (200 μm). The *in situ* electrogenerated Cu(I) species reacts readily with O₂ to form a transient Cu(II)-superoxo species which can be stabilized at low temperature and displays a typical UV-Vis signature at $\lambda_{\text{max}} = 400$ nm and 592 nm. Reprinted with permission from [135], copyright (2017) American Chemical Society.

Similar techniques were used by Belle and co-workers in 2018 for the study of an unsymmetrical phenoxo and hydroxo-bridge dicopper(II) complex (Figure 17), considered as synthetic models of particulate methane monooxygenases [136]. The authors investigated the monoelectronic oxidation of the complex in DMF at $T = 213$ K since CV was reversible only at this temperature. Time-resolved UV-Vis spectroelectrochemistry was used to probe the formation of a mixed-valent Cu(II)Cu(III) species upon oxidation. A band at $\lambda_{\text{max}} = 386$ nm was detected through CV scanning and disappeared when sweeping back to the initial potential (Figure 17). According to TD-DFT analysis, this band was ascribed to a ligand-to-metal charge transfer essentially between the phenoxido ligand and the Cu(III)

ion, consistent with an oxidation process occurring on one of the metal center. Room temperature study suggested that this mixed-valent species could further perform hydrogen atom abstraction.

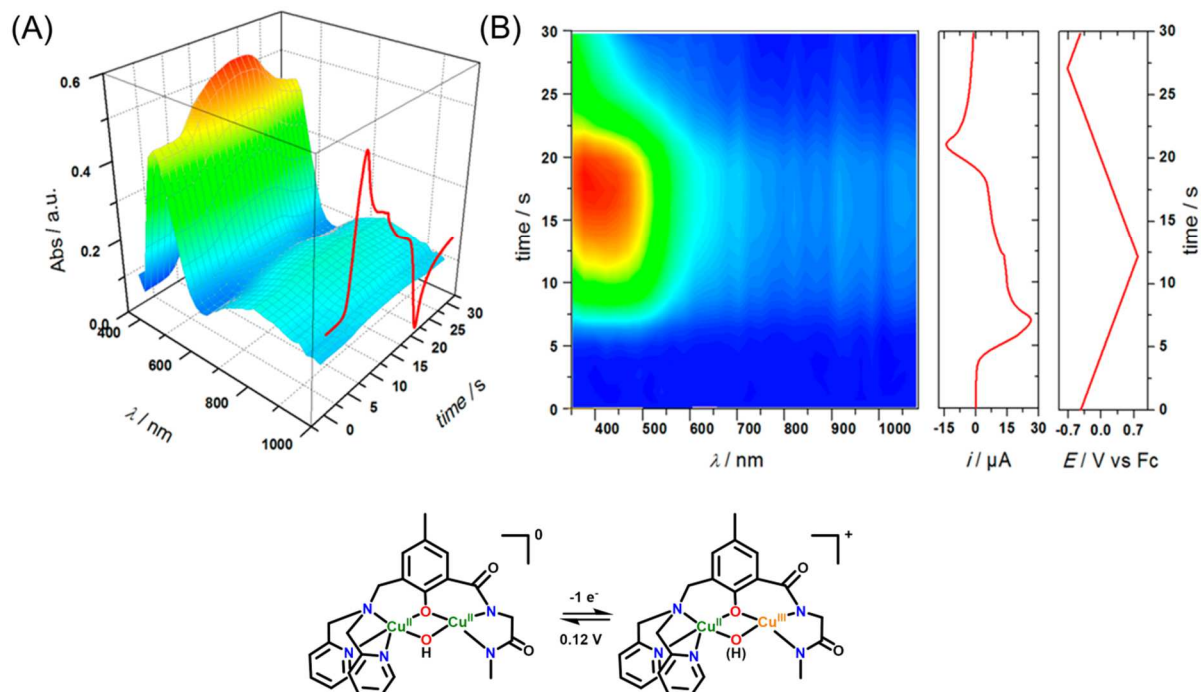


Figure 17. A) 3D UV-Vis spectroscopic monitoring of the electrochemical mono-oxidation of the dicopper μ -hydroxo complex in 0.1 M $\text{NBu}_4\text{ClO}_4/\text{DMF}$ at $T = 213$ K under thin-layer conditions (200 μm). The red curve represents the current intensity (i) response (*vs.* time) upon variation of potential; B) 2D differential (*vs.* initial spectrum) spectroscopic response of the dicopper complex upon electrochemical oxidation. The red curves on the right panels represents the variation of the current intensity (i) and potential (E) with time. Reprinted with permission from [136], copyright (2018) American Chemical Society.

Very recently, Hartl *et al.* investigated the electrochemical properties of the complexes $[\text{Re}(3,3\text{-DHBPY})(\text{CO})_3\text{Cl}]$ and $[\text{Re}(3,3\text{-DHBPY})(\text{CO})_3(\text{PrCN})]^+$ (3,3'-DHBPY = 3,3'-dihydroxy-2,2'-bipyridine), which are moderately active catalysts for the electrochemical reduction of CO_2 [153]. The authors particularly aimed at showing the influence of the hydroxy groups located on the 3,3' (*vs.* 4,4') positions of the bipyridine ligand on the mechanistic pathways. Electrochemistry and IR spectroelectrochemistry with an OTLLE cell were carried out at room and low temperature to decipher the mechanisms, and proton exchange associated to electron transfer. Analysis of the IR spectra obtained at $T = 223$ K, 258 K and 298 K in butyronitrile of both rhenium complexes allowed the characterization of several transient species. Indeed, at $T = 223$ K, the reduction of the mono-deprotonated species $[\text{Re}(3,3'\text{-DHBPY-H}^+)(\text{CO})_3(\text{Cl})]^-$ and $[\text{Re}(3,3'\text{-DHBPY-H}^+)(\text{CO})_3(\text{PrCN})]$ led to

the characterization of the transient double-deprotonated intermediates $[\text{Re}(3,3'\text{-DHBPY-2H}^+)(\text{CO})_3(\text{Cl})]^{2-}$ and $[\text{Re}(3,3'\text{-DHBPY-2H}^+)(\text{CO})_3(\text{PrCN})]^-$, respectively. Other species resulting from a net-zero-electron, electron transfer catalytic (ETC) process were also detected, according to the mechanistic pathway shown in Figure 18. Increasing the temperature to $T = 258 \text{ K}$ induced the cleavage of the Re-Cl bond for the chloride-based complex. Moreover, species resulting from the ETC process were dominantly detected.

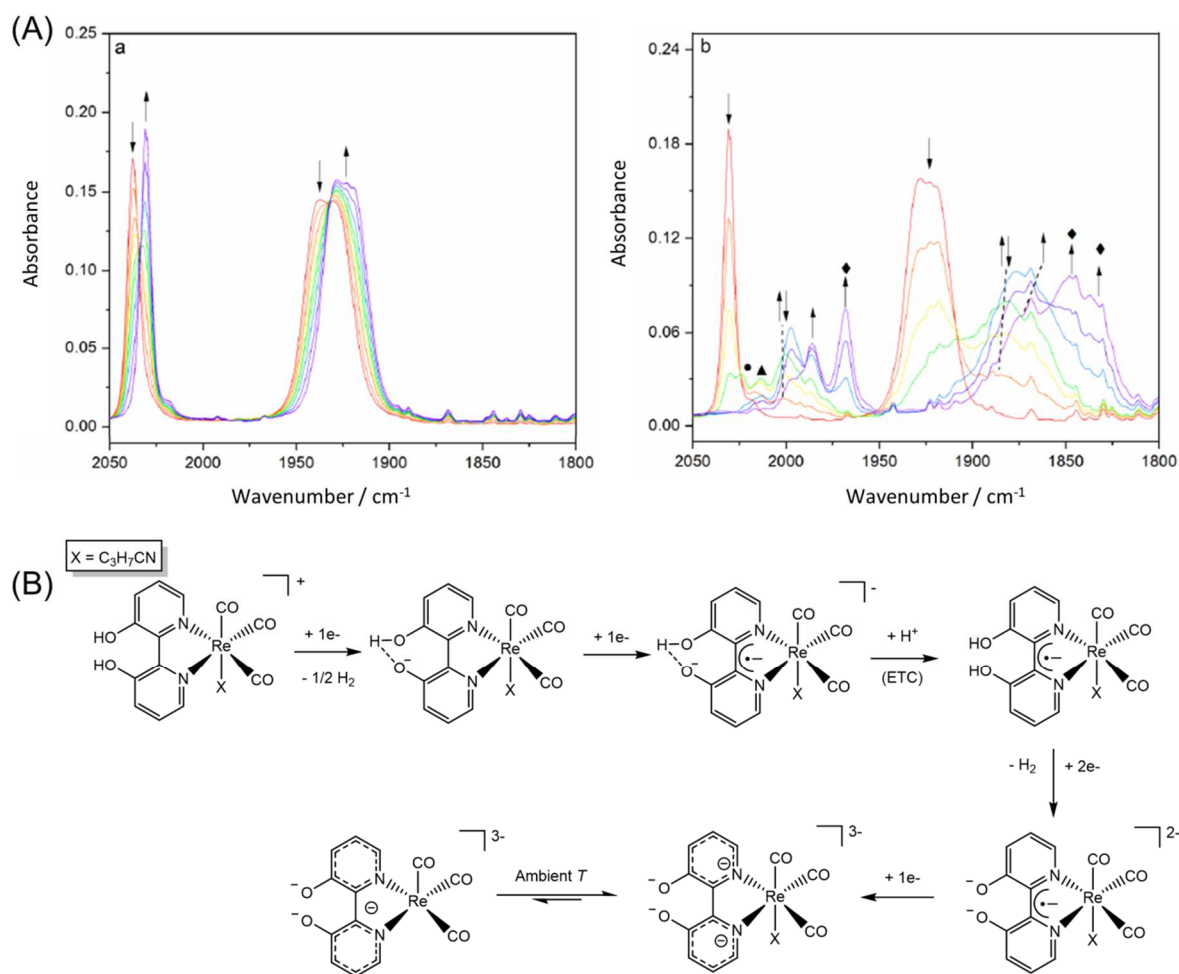


Figure 18. A) Low-temperature ($T = 223 \text{ K}$) IR spectroelectrochemistry of the reduction of $[\text{Re}(3,3'\text{-DHBPY})(\text{CO})_3(\text{PrCN})]^+$ (\downarrow) in $0.1 \text{ M NBu}_4\text{PF}_6/\text{PrCN}$ (a) for the first reduction with conversion of the parent complex to $[\text{Re}(3,3'\text{-DHBPY-H}^+)(\text{CO})_3(\text{PrCN})]$ (\uparrow), and (b) for the second reduction with transformation of $[\text{Re}(3,3'\text{-DHBPY-H}^+)(\text{CO})_3(\text{PrCN})]$ (\downarrow) to a mixture of products with dominating $[\text{Re}(3,3'\text{-DHBPY})(\text{CO})_3(\text{PrCN})]$ ($\uparrow\downarrow$) formed in an ETC step. The small band labelled with \bullet may belong to marginal reductively double-deprotonated $[\text{Re}(3,3'\text{-DHBPY-2H}^+)(\text{CO})_3(\text{PrCN})]^-$. Its $1e^-$ and $2e^-$ reduced forms, $[\text{Re}(3,3'\text{-DHBPY}\bullet\text{-2H}^+)(\text{CO})_3(\text{PrCN})]^{2-}$ (\uparrow) and $[\text{Re}(3,3'\text{-DHBPY}_2\text{-2H}^+)(\text{CO})_3(\text{PrCN})]^{3-}$ (\blacklozenge), terminate the cathodic path. The label \blacktriangle denotes an unassigned reduced intermediate. B) Proposed mechanism for the complex. Reprinted with permission from [153], copyright (2020) American Chemical Society.

Table 5. Selected examples of low-temperature spectroelectrochemical studies (in chronological order).

Compound	T_{low}/K	Spectroscopic method	Aim	Ref.
[Hg(cyclam)] ²⁺	193	UV-Vis, EPR	Characterization of Hg(III) species	[50]
[Fe(CO) ₃ (PPh ₃) ₂]	223	EPR	Characterization of [Fe(CO) ₃ (PPh ₃) ₂] ⁺	[104]
[Cr(CO) ₄ (PPh ₃) ₂]	273	EPR	Characterization of [Cr(CO) ₄ (PPh ₃) ₂] ⁺	[105]
[Cr(CO) ₃ (PPh ₃) ₃]	200	EPR	Rate of isomerization of <i>fac-mer</i> [Cr(CO) ₃ (PPh ₃) ₃] ⁺	[106]
[Cr(mnt) ₃] ³⁻	253	IR	Characterization of [Cr(mnt) ₃] ⁻ and [Cr(mnt) ₃] ²⁻	[97]
[(OEP)Ir(CO)Cl]	223	EPR	Characterization of [(OEP)Ir(CO)Cl] ⁺	[103]
[RuCl ₃ (CH ₃ CN) ₃]	238	UV-Vis	Characterization of [RuCl ₃ (CH ₃ CN) ₃] ⁺	[91]
[Re ₂ Cl ₉] ⁻	188	UV-Vis	Characterization of [Re ₂ Cl ₉] ²⁻ and [Re ₂ Cl ₉] ³⁻	[69]
[(mesitylene)W(CO) ₃]	238	IR	Characterization of [(mesitylene)W(CO) ₃ (MeCN)] ⁺	[66]
[Re ₂ (NCS) ₈] ²⁻	215	UV-Vis	Characterization of [Re ₂ (NCS) ₈] ³⁻ and [Re ₂ (NCS) ₈] ⁻	[139]
[Mn(CO) ₃ (DBCat)] ⁻	223	IR, UV-Vis	Characterization of [Mn(CO) ₃ (H ₂ O)(DBCQ)] and [Ru(PrCN)(Me)(CO) ₂ (iPr-DAB)] ^o	[93]
[RuI(Me)(CO) ₂ (iPr-DAB)] ⁻	183			
[Mo(mnt) ₃] ²⁻	253	IR	Characterization of [Mo(mnt) ₃] ⁴⁺	[96]
[Ru ₁₀ (μ-H)(μ ₆ -C)(CO) ₂₄] [Ru ₁₀ (μ ₆ -C)(CO) ₂₄]	213	UV-Vis	Characterization of transient reduced species	[140]
[Mn(X)(CO) ₃ (iPr-DAB)] (X=Br, Cl, Bz)	198	IR, UV-Vis	Characterization of [Mn(PrCN)(CO) ₃ (iPr-DAB)] ^o radical anion.	[154]
[TcNX ₄] ⁻ [TcOX ₄] ⁻ (X = Cl or Br)	218	UV-Vis	Characterization of [TcNX ₄] ²⁻ and [TcNO ₄] ²⁻	[141]
[Cr(CO) ₃ (η ⁶ -C ₁₆ H ₁₆ -1,4)]	213	IR, EPR	Characterization of [Cr(CO) ₃ (η ⁶ -C ₁₆ H ₁₆ -1,4)] ^{o+} radical cation	[142]
[Re(Bn)(CO) ₃ (dmb)]	223	EPR, UV-Vis	Characterization of [Re(Bn)(CO) ₃ (dmb)] ^{o-} radical anion	[111]
N,N,N',N'-Tetramethyl-1,4-	260	EPR-UV-Vis-NIR	Characterization of the	[117]

phenylendiamine			radical cation by multi-spectroelectrochemistry	
[Fe(CO) ₃ (nbd)]	258	IR	Characterization of [Fe(CO) ₃ (nbd)] ^{•+} radical anion	[98]
[Os(bpy)(CO) ₂ Cl ₂]	273	IR	Characterization of [Os(bpy)(CO) ₂ Cl ₂] ⁺	[155]
[RhCl(CO)(iPr ₂ Ph-bian)]	193	IR, EPR	Characterization of [RhCl(CO)(iPr ₂ Ph-bian)] ⁻ , [RhCl(CO)(iPr ₂ Ph-bian)] ²⁻ and [Rh(CO)(iPr ₂ Ph-bian)] ⁻	[95]
[Re(bopy)(bpy)(CO) ₃] ⁺	223	IR	Characterization of [Re(bopy)(bpy)(CO) ₃], [Re(bopy)(bpy [•])(CO) ₃] ⁻ , [Re(PrCN)(bpy) ₂ (CO) ₃] ²⁻	[156]
[Mn(T(<i>p</i> -OMe)P)(NO)(1-MeIm)]	195	IR	Characterization of [Mn(T(<i>p</i> -OMe)P)(NO)(1-MeIm)] ⁺	[102]
[W(CO) ₄ (nbd) ₂] [W(CO) ₄ (ethene) ₂]	243	IR	Characterization of [W(CO) ₄ (nbd) ₂] ^{•-} and [W(CO) ₄ (ethene) ₂] ^{•-}	[157]
<i>p</i> -(Fc-CH=CH) ₂ Bz	203	IR	Characterization of [<i>p</i> -(Fc-CH=CH) ₂ Bz] ⁺	[126]
[Fe(Cp)] ²⁻ [Rh(cod)] ²⁻ [Fe(Cp)Rh(cod)] ⁻	248	UV-Vis	Characterization of transient mixed-valent species in the NIR domain	[127]
[Ferrocenyl-indenyl]Rh(L) (L=cod, nbd)	253	UV-Vis	Characterization of transient mixed-valent species in the NIR domain	[158]
[(TMP)Fe ^{IV} O]	213	UV-Vis	Characterization of one and two-electron oxidized species of [(TMP)Fe ^{IV} O]	[92]
[Mo(CO) ₂ (^{mes} DAB ^H) ₂]	195	IR	Characterization of [Mo(CO) ₂ (^{mes} DAB ^H) ₂] ⁺	[159]
[M(L)(<i>p</i> -cymene)] (M=Os, Ru) (L=4,6-di-tert-butyl-N-aryl-o-amidophenolate)	223	UV-Vis	Characterization of [M(L)(<i>p</i> -cymene)] ⁺ and [M(L)(<i>p</i> -cymene)] ²⁺	[160]
[Mo(CO) ₂ (η ³ -allyl)(bpy)(NCS)]	183	IR	Characterization of [Mo(CO) ₂ (η ³ -allyl)(bpy)(NCS)] ⁺ , [Mo(CO) ₂ (η ³ -allyl)(bpy)(NCS)] ⁻ and [Mo(CO) ₂ (η ³ -allyl)(bpy)(PrCN)] ⁻	[148]
[Os(CO)(bpy)Cl ₃]	213	IR	Characterization of [Os(CO)(bpy)Cl ₃] ⁻ , [Os(CO)(bpy)Cl ₃] ²⁻ and [Os(CO)(bpy)(PrCN)] ⁻	[149]
[Cu(calix[6]amidotren)] ²⁺	213	UV-Vis	Characterization of	[135]

[Cu ₂ (UNO)(O ₂)] ²⁺	183	UV-Vis	[Cu(calix[6]amidotren)(O ₂)] ⁺	Characterization of [Cu ₂ (UNO)(O ₂)] ⁺ .	[121]
[Mo(allyl)(CO) ₂ (dmbipy)(NCS)]	223	IR		Characterization of mono and bis-reduced species	[152]
[Cu ₂ (BPAPhOBA)(μ-OH)] ²⁺	213	UV-Vis		Characterization of the mixed-valent oxidized species	[136]
1,1'-diphenyl-2-cymantrenylbutene	273	IR		Characterization of mono and bis-oxidized species	[83]
[Re(3,3'-DHBPY)-(CO) ₃ Cl]	223	IR		Characterization of mono and bis-reduced species.	[153]

4. Conclusions and outlooks

This review has focused on the different aspects of low-temperature electrochemistry and spectroelectrochemistry applied for organometallic and coordination compounds. As shown by the cited examples, cryo-electrochemistry can be a powerful tool allowing not only the determination of the thermodynamics and kinetics of electron transfer or associated chemical reactions, but also for the redox characterization of electroactive species which cannot be stabilized at room temperature. Furthermore, when coupled to spectroscopic methods, it affords the spectroscopic identification of *in situ*-generated oxidized or reduced species in a time-resolved manner. Such a benefit is of high interest for rationalizing mechanistic pathways through the characterization of intermediate compounds, with the help of computational studies. Although various cryo-electrochemical and spectroelectrochemical set-ups have been well developed for the last 40 years, the number of reported studies using these approaches remains finally scarce. One main reason is that commercial (spectro)electrochemical systems for room and low-temperature studies remain expensive, and the rare set-ups (in EPR and UV-Vis spectroscopy) which are available are often limited in terms of temperature range. Moreover, problems arising when the temperature is decreased, such as high ohmic drop, water condensation or solvent freezing may not contribute to make cryo-electrochemistry and spectroelectrochemistry so attractive at a first glance. Still, much progress has to be made by researchers and industries to generate (spectro)electrochemical packages which could be performant and easy to handle for low-*T* investigations.

At the laboratory scale, a wide choice of possibilities is available for the research community. As mentioned in this review, spectroelectrochemical techniques involving UV-Vis-NIR, IR or EPR spectroscopies have been the most used for low-temperature studies (and also for ambient conditions). Nevertheless, the *in situ* coupling of electrochemical methods with other spectroscopy and microscopy techniques such as fluorescence, Resonance Raman, NMR, XAS, SECM, AFM, to cite a few, remains

of high interest when used at low temperature because it provides valuable information on the redox species formed at the electrode surface. Some spectroelectrochemical set-ups using these techniques have already been described. For instance, coupled electrochemical ^1H NMR studies of a thiophene derivative were reported by Dunsch and co-workers in 2010 for a temperature range [161]. The specific design of the cell allowed the characterization of a π -dimer via the cation generated in the first electron transfer as well as the formation of a σ -dimer by a follow-up reaction of the dication generated in the second oxidation step. In another example, tip-enhanced Raman spectroscopy (TERS) was used at ultra-low temperatures (90 K) to selectively probe the intramolecular vibrational coupling of single-molecule deposited by spin coating on an Au/Si surface [162]. Luminescence-based innovative devices have also been designed with the help of a low- T OTTLE cell [163]. More generally, the multi-spectroelectrochemistry concept developed by Dunsch *et al.* which results from the combination of electrochemistry with several spectroscopic methods for *in situ* characterization is highly promising for usage at low temperatures, even if it may require a high degree of technical sophistication [115]. The on-going miniaturization of many electrochemical systems (arrays, chips, screen-printed electrodes...) coupled to the significant progress of various spectroscopic set-ups (faster acquisition, better sensitivity, fiber optic transmission...) give the opportunity today to push towards the generation of novel cryo-electrochemical and spectroelectrochemical devices for various applications (catalysis, electrochromic sensors, energy conversion...) [164].

Author information

*Corresponding authors

Isidoro López: isilopmarin@gmail.com. ORCID: 0000-0002-6014-0078

Nicolas Le Poul: nicolas.lepoul@univ-brest.fr. ORCID: 0000-0002-5915-3760

Notes

The authors declare no competing financial interest.

Acknowledgments

Financial support by ANR-13-BSO7-0018, Conseil Général du Finistère, Université de Bretagne Occidentale and Campus France (Prestige grant number 2015-2-0019 for I. L.-M.).

References

- [1] W. Kaim, A. Klein, Spectroelectrochemistry, RSC Publishing, 2008.
- [2] W. Kaim, J. Fiedler, Chem. Soc. Rev., 38 (2009) 3373-3382.
- [3] J.J.A. Lozeman, P. Fuhrer, W. Olthuis, M. Odijk, Analyst, 145 (2020) 2482-2509.
- [4] D.H. Evans, S.A. Lerke, in Laboratory techniques in electroanalytical chemistry (Eds P. T. Kissinger, W. R. Heineman), Marcel Dekker, (1996) 487-510.

- [5] R.P. Van Duyne, C.N. Reilly, *Anal. Chem.*, 44 (1972) 142-152.
- [6] L. Rand, C.S. Rao, *J. Org. Chem.*, 33 (1968) 2704-2708.
- [7] B.G. Dekker, M. Sluyters-Rehbach, J.H. Sluyters, *J. Electroanal. Chem.*, 21 (1969) 137-147.
- [8] F.F. Gadallah, R.M. Elfson, *J. Org. Chem.*, 34 (1969) 3339-3338.
- [9] R.A. Meinzer, D.W. Pratt, R.J. Myers, *J. Am. Chem. Soc.*, 91 (1969) 6623-6625.
- [10] R.J. Wilson, L.F. Warren Jr., M.F. Hawthorne, *J. Am. Chem. Soc.*, 91 (1969) 758-759.
- [11] L.L. Miller, E.A. Mayeda, *J. Am. Chem. Soc.*, 92 (1970) 5818-5819.
- [12] F. Gaillard, E. Levillain, *J. Electroanal. Chem.*, 398 (1995) 77-87.
- [13] T. Nagaoka, S. Okazaki, *Anal. Chem.*, 55 (1983) 1836-1837.
- [14] L.S. Curtin, S.R. Peck, L.M. Tender, R.W. Murray, G.K. Rowe, S.E. Creager, *Anal. Chem.*, 65 (1993) 386-392.
- [15] J.N. Richardson, J. Harvey, R.W. Murray, *J. Phys. Chem.*, 98 (1994) 13396-13402.
- [16] S.J. Green, D.R. Rosseinsky, M.J. Toohey, *J. Am. Chem. Soc.*, 114 (1992) 9702-9704.
- [17] S.J. Green, D.R. Rosseinsky, M.J. Toohey, *J. Chem. Soc., Chem. Commun.*, (1994) 325.
- [18] S.J. Green, D.R. Rosseinsky, D.C. Sinclair, *J. Chem. Soc., Chem. Commun.*, (1994) 1421-1422.
- [19] S.J. Green, D.R. Rosseinsky, M.J. Toohey, *J. Electrochem. Soc.*, 142 (1995) 2272-2277.
- [20] N. Le Poul, S.J. Green, Y. Le Mest, *J. Electroanal. Chem.*, 596 (2006) 47-56.
- [21] Z.-X. Huang, S. Yang, J.-W. Guo, S.-H. Wu, J.-J. Sun, G.-N. Chen, *Electrochem. Commun.*, 48 (2014) 107-110.
- [22] K.M. O'Connell, D.H. Evans, *J. Am. Chem. Soc.*, 105 (1983) 1473-1481.
- [23] K.M. Kadish, K. Das, D. Schaeper, C.L. Merrill, B.R. Welch, L.J. Wilson, *Inorg. Chem.*, 19 (1980) 2816-2821.
- [24] G. Farnia, F. Marcuzzi, G. Melloni, G. Sandona, *J. Am. Chem. Soc.*, 106 (1984) 6503-6512.
- [25] W.J. Bowyer, D.H. Evans, *J. Org. Chem.*, 53 (1988) 5234-5239.
- [26] G. Farnia, G. Sandoni, F. Marcuzzi, G. Melloni, *J. Chem. Soc., Perkin Trans. 2*, (1988) 247-254.
- [27] W.J. Bowyer, E.E. Engelman, D.H. Evans, *J. Electroanal. Chem.*, 262 (1989) 67-82.
- [28] C.E.D. Chidsey, *Science*, 251 (1991) 919-922.
- [29] M.T. Carter, G.K. Rowe, J.N. Richardson, L.M. Tender, R.H. Terrill, R.W. Murray, *J. Am. Chem. Soc.*, 117 (1995) 2896-2899.
- [30] J.N. Richardson, S.R. Peck, L.S. Curtin, L.M. Tender, R.H. Terrill, M.T. Carter, R.W. Murray, G.K. Rowe, S.E. Creager, *J. Phys. Chem.*, 99 (1995) 766-772.
- [31] S. Ching, J.T. McDevitt, S.R. Peck, R.W. Murray *J. Electrochem. Soc.*, 138 (1991) 2308-2315.
- [32] A.J. Klein, D.H. Evans, *J. Am. Chem. Soc.*, 101 (1979) 757-758.
- [33] N.J. Stone, D.A. Sweigart, A.M. Bond, *Organometallics*, 5 (1986) 2553-2555.
- [34] E. Anxolabéhère, D. Lexa, M. Momenteau, J.M. Saveant, *J. Phys. Chem.*, 96 (1992) 9348-9352.
- [35] Y. Liu, A.H. Flood, P.A. Bonvallet, S.A. Vignon, B.H. Northrop, H.R. Tseng, J.O. Jeppesen, T.J. Huang, B. Brough, M. Baller, S. Magonov, S.D. Solares, W.A. Goddard, C.M. Ho, J.F. Stoddart, *J. Am. Chem. Soc.*, 127 (2005) 9745-9759.
- [36] C. Hamacher, N. Hurkes, A. Kaiser, A. Klein, A. Schuren, *Inorg. Chem.*, 48 (2009) 9947-9951.
- [37] J.C. Swarts, A. Nafady, J.H. Roudebush, S. Trupia, W.E. Geiger, *Inorg. Chem.*, 48 (2009) 2156-2165.
- [38] I. Engelhardt, R. Speck, J. Inche, H.S. Khalil, M. Ebert, W.J. Lorenz, G. Saemann-Ischenko, M.W. Breiter, *Electrochim. Acta*, 37 (1992) 2129-2136.
- [39] M. Akani, A. Froese, G. Staikov, W.J. Lorenz, M. Röhner, R. Hopfengärtner, G. Saemann-Ischenko, *Physica C*, 245 (1995) 131-138.
- [40] J.T. McDevitt, R.W. Murray, S.I. Shah, *J. Electrochem. Soc.*, 138 (1991) 1346-1350.
- [41] S.R. Peck, L.S. Curtin, J.T. McDevitt, R.W. Murray, J.P. Collman, W.A. Little, T. Zetterer, H.M. Duan, C. Dong, A.M. Hermann, *J. Am. Chem. Soc.*, 114 (1992) 6771-6775.
- [42] S.J. Green, D.R. Rosseinsky, D.R. Rosseinsky, A.L. Kharlanov, J. Paul Attfield, *Chem. Commun.*, (1998) 1215-1216.
- [43] R.O. Gollmar, J.T. McDevitt, R.W. Murray, J.P. Collman, G.T. Yee, L.W. A., *J. Electrochem. Soc.*, 136 (1989) 3696-3701.
- [44] S.J. Green, N. Le Poul, P.P. Edwards, G. Peacock, *J. Am. Chem. Soc.*, 125 (2003) 3686-3687.
- [45] S.R. Peck, L.S. Curtin, L.M. Tender, M.T. Carter, R.H. Terrill, R.W. Murray, J.P. Collman, W.A. Little, H.M. Duan, *J. Am. Chem. Soc.*, 117 (1995) 1121-1126.
- [46] N. Le Poul, S.J. Green, J.P. Attfield, *Chem. Commun.*, (2003) 638-639.
- [47] L.K. Safford, M.J. Weaver, *J. Electroanal. Chem.*, 331 (1992) 857-876.
- [48] A.M. Bond, M. Fleischmann, J. Robinson, *J. Electroanal. Chem.*, 180 (1984) 257-263.
- [49] A. Evans, M.I. Montenegro, D. Pletcher, *Electrochem. Commun.*, 3 (2001) 514-518.
- [50] R.L. Deming, A.L. Allred, A.R. Dahl, A.W. Herlinger, M.O. Kestner, *J. Am. Chem. Soc.*, 98 (1976) 4132-4137.

- [51] D.H. Evans, R.W. Busch, *J. Am. Chem. Soc.*, 104 (1982) 5057-5062.
- [52] N. Fietkau, C.A. Paddon, F.L. Bhatti, T.J. Donohoe, R.G. Compton, *J. Electroanal. Chem.*, 593 (2006) 131-141.
- [53] M. Sakagami, T. Sasamori, H. Sakai, Y. Furukawa, N. Tokitoh, *Bull. Chem. Soc. Jpn.*, 86 (2013) 1132-1143.
- [54] U. Stimming, W. Schmickler, *J. Electroanal. Chem.*, 150 (1983) 125-131.
- [55] T. Brülle, O. Schneider, U. Stimming, *Zeit. Physik. Chem.*, 226 (2012) 919-934.
- [56] U. Frese, U. Stimming, *J. Electroanal. Chem.*, 198 (1986) 409-416.
- [57] A.M. Bond, V.B. Pfund, *J. Electroanal. Chem.*, 335 (1992) 281-295.
- [58] K. Tanaka, R. Tamamushi, *J. Electroanal. Chem.*, 380 (1995) 279-282.
- [59] A. Pinkowski, J. Doneit, K. Juttner, W.J. Lorenz, G. Saemann-Isschenko, M. Breiter, *Europhys. Lett.*, 9 (1989) 269-275.
- [60] A. Pinkowski, J. Doneit, K. Juttner, W.J. Lorenz, G. Saemann-Isschenko, T. Zetterer, M. Breiter, *Physica C*, 162 (1989) 1039-1040.
- [61] W.J. Lorenz, G. Saemann-Isschenko, M.W. Breiter, *Modern aspects of electrochemistry*, Plenum Press, 1995.
- [62] A. Pinkowski, K. Juttner, W.J. Lorenz, G. Saemann-Isschenko, M. Breiter, *J. Electroanal. Chem.*, 286 (1990) 253-256.
- [63] J.T. McDevitt, S. Ching, M. Sullivan, R.W. Murray, *J. Am. Chem. Soc.*, 111 (1989) 4528-4529.
- [64] A.M. Bond, J.A. Bowden, R. Colton, *Inorg. Chem.*, 13 (1974) 602-608.
- [65] S.F. Nelsen, E.L. Clennan, D.H. Evans, *J. Am. Chem. Soc.*, 100 (1978) 4012-4019.
- [66] Y. Zhang, D.K. Gosser, P.H. Rieger, D.A. Sweigart, *J. Am. Chem. Soc.*, 113 (1991) 4062-4068.
- [67] D. Dubois, G. Moninot, W. Kutner, M.T. Jones, K.M. Kadish, *J. Phys. Chem.*, 96 (1992) 7137-7145.
- [68] A.M. Bond, D.A. Sweigart, *Inorg. Chim. Acta*, 123 (1986) 167-173.
- [69] G.A. Heath, R.G. Raptis, *Inorg. Chem.*, 30 (1991) 4106-4108.
- [70] P. O'Brien, D.A. Sweigart, *J. Chem. Soc., Chem. Commun.*, (1986) 198-200.
- [71] J. Mortensen, J. Heinze, *Angew. Chem. Int. Ed. Engl.*, 23 (1984) 84-85.
- [72] A.S. Baranski, K. Winkler, W.R. Fawcett, *J. Electroanal. Chem.*, 313 (1991) 367-375.
- [73] E.F. Dalton, S. Ching, R.W. Murray, *Inorg. Chem.*, 30 (1991) 2642-2648.
- [74] R. Baron, N.M. Kershaw, T.J. Donohoe, R.G. Compton, *J. Phys. Org. Chem.*, 22 (2009) 247-253.
- [75] K.M. Kadish, C.L. Yao, J.E. Anderson, P. Cocolios, *Inorg. Chem.*, 24 (1985) 4515-4520.
- [76] F.J. Del Campo, A. Neudeck, R.G. Compton, F. Marken, *J. Electroanal. Chem.*, 477 (1999) 71-78.
- [77] F.J. Del Campo, A. Neudeck, R.G. Compton, F. Marken, S.D. Bull, S.G. Davies, *J. Electroanal. Chem.*, 507 (2001) 144-151.
- [78] R.L. Birke, Q. Huang, T. Spataru, D.K. Gosser, *J. Am. Chem. Soc.*, 128 (2006) 1922-1936.
- [79] S.F. Nelsen, D.L. Kapp, F. Gerson, J. Lopez, *J. Am. Chem. Soc.*, 108 (1986) 1027-1032.
- [80] Q. Xie, E. Perez-Cordero, L. Echegoyen, *J. Am. Chem. Soc.*, 114 (1992) 3978-3980.
- [81] Y. Ohsawa, T. Saji, *J. Chem. Soc., Chem. Commun.*, (1992) 781-782.
- [82] D.R. Laws, R.M. Bullock, R. Lee, K.-W. Huang, W.E. Geiger, *Organometallics*, 33 (2014) 4716-4728.
- [83] K. Wu, J.Y. Park, R. Al-Saadon, H. Nam, Y. Lee, S. Top, G. Jaouen, M.-H. Baik, W.E. Geiger, *Organometallics*, 37 (2018) 1910-1918.
- [84] W.A. Nevin, W. Liu, *Anal. Sci.*, 4 (1988) 559-563.
- [85] M.J. Shaw, W.E. Geiger, *Organometallics*, 15 (1996) 13-15.
- [86] R.S. Czernuszewicz, K.A. Macor, *J. Raman Spectr.*, 19 (1988) 553-557.
- [87] D.A. Fiedler, M. Koppenol, A.M. Bond, *J. Electrochem. Soc.*, 142 (1995) 862-867.
- [88] R.W. Murray, W.R. Heineman, G.W. O'Dom, *Anal. Chem.*, 39 (2002) 1666-1668.
- [89] J.P. Bullock, D.C. Boyd, K.R. Mann, *Inorg. Chem.*, 26 (1987) 3084-3086.
- [90] C. Gueutin, D. Lexa, *Electroanalysis*, 8 (1996) 1029-1033.
- [91] C.M. Duff, G.A. Heath, *Inorg. Chem.*, 30 (1991) 2528-2535.
- [92] A. Takahashi, T. Kurahashi, H. Fujii, *Inorg. Chem.*, 50 (2011) 6922-6928.
- [93] F. Hartl, H. Luyten, H.A. Nieuwenhuis, G.C. Schoemaker, *Appl. Spectrosc.*, 48 (1994) 1522-1528.
- [94] M. Krejčík, M. Daněk, F. Hartl, *J. Electroanal. Chem.*, 317 (1991) 179-187.
- [95] T. Mahabiersing, H. luyten, R.C. Nieuwendam, F. Hartl, *Coll. Czech. Chem. Commun.*, 68 (2003) 1687-1709.
- [96] S.P. Best, S.A. Ciniawsky, D.G. Humphrey, *J. Chem. Soc., Dalton Trans.*, (1996) 2945-2949.
- [97] S.P. Best, R.J.H. Clark, R.C.S. McQueen, R.P. Cooney, *Rev. Sci. Instr.*, 58 (1987) 2071-2074.
- [98] I.S. Zavarine, C.P. Kubiak, *J. Electroanal. Chem.*, 495 (2001) 106-109.
- [99] C.W. Machan, M.D. Sampson, S.A. Chabolla, T. Dang, C.P. Kubiak, *Organometallics*, 33 (2014) 4550-4559.
- [100] J. Salbeck, *J. Electroanal. Chem.*, 340 (1992) 169-195.

- [101] M.J. Shaw, R.L. Henson, S.E. Houk, J.W. Westhoff, M.W. Jones, G.B. Richter-Addo, *J. Electroanal. Chem.*, 534 (2002) 47-53.
- [102] Z.N. Zahran, M.J. Shaw, M.A. Khan, G.B. Richter-Addo, *Inorg. Chem.*, 45 (2006) 2661-2668.
- [103] X.H. Mu, K.M. Kadish, *Electroanalysis*, 2 (1990) 15-20.
- [104] R.N. Bagchi, A.M. Bond, C.L. Heggie, T.L. Henderson, E. Mocellin, R.A. Seikel, *Inorg. Chem.*, 22 (1983) 3007-3012.
- [105] R.N. Bagchi, A.M. Bond, G. Brain, R. Colton, T.L.E. Henderson, J.E. Kevekordes, *Organometallics*, 3 (1984) 4-9.
- [106] R.N. Bagchi, A.M. Bond, R. Colton, *J. Electroanal. Chem.*, 199 (1986) 297-309.
- [107] R.N. Bagchi, A.M. Bond, F. Scholz, R. Stösser, *J. Electroanal. Chem.*, 245 (1988) 105-112.
- [108] R.N. Bagchi, A.M. Bond, F. Schulz, *J. Electroanal. Chem.*, 252 (1988) 259-267.
- [109] R.N. Bagchi, A.M. Bond, F. Scholz, *Electroanalysis*, 1 (1989) 1-11.
- [110] R.D. Allendoerfer, G.A. Martinchek, S. Bruckenstein, *Anal. Chem.*, 47 (1975) 890-894.
- [111] F. Hartl, R.P. Groenestein, T. Mahabiersing, *Coll. Czech. Chem. Commun.*, 66 (2001) 52-66.
- [112] A.J. Wain, R.G. Compton, *J. Electroanal. Chem.*, 587 (2006) 203-212.
- [113] A.J. Wain, R.G. Compton, R. Le Roux, S. Matthews, A.C. Fisher, *Anal. Chem.*, 79 (2007) 1865-1873.
- [114] A. Petr, L. Dunsch, A. Neudeck, *J. Electroanal. Chem.*, 412 (1996) 153-158.
- [115] L. Dunsch, *J. Sol. St. Electrochem.*, 15 (2011) 1631-1646.
- [116] P. Rapta, L. Kress, P. Hapiot, L. Dunsch, *Physical chemistry chemical physics : PCCP*, 4 (2002) 4181-4185.
- [117] P. Rapta, L. Dunsch, *J. Electroanal. Chem.*, 507 (2001) 287-292.
- [118] J.T. McDevitt, M. Longmire, R.O. Gollmar, J.C. Jernigan, E.F. Dalton, R. McCarley, R.W. Murray, W.A. Little, G.T. Yee, M.J. Holcomb, J.E. Hutchinson, J.P. Collman, *J. Electroanal. Chem.*, 243 (1988) 465-474.
- [119] G. Ali, P.E. VanNatta, D.A. Ramirez, K.M. Light, M.T. Kieber-Emmons, *J. Am. Chem. Soc.*, 139 (2017) 18448-18451.
- [120] N. Kindermann, C.J. Gunes, S. Dechert, F. Meyer, *J. Am. Chem. Soc.*, 139 (2017) 9831-9834.
- [121] I. Lopez, R. Cao, D.A. Quist, K.D. Karlin, N. Le Poul, *Chem. Eur. J.*, 23 (2017) 18314-18319.
- [122] T.J. Zerk, C.T. Saouma, J.M. Mayer, W.B. Tolman, *Inorg. Chem.*, 58 (2019) 14151-14158.
- [123] J. Rittle, J.C. Peters, *J. Am. Chem. Soc.*, 139 (2017) 3161-3170.
- [124] L. Tender, M.T. Carter, R.W. Murray, *Anal. Chem.*, 66 (1994) 3173-3181.
- [125] J. Shearer, C.X. Zhang, L.N. Zakharov, A.L. Rheingold, K.D. Karlin, *J. Am. Chem. Soc.*, 127 (2005) 5469-5483.
- [126] P. Liu, B. Jin, F. Cheng, *J. Electroanal. Chem.*, 603 (2007) 269-274.
- [127] S. Santi, L. Orian, C. Durante, E.Z. Bencze, A. Bisello, A. Donoli, A. Ceccon, F. Benetollo, L. Crociani, *Chem. Eur. J.*, 13 (2007) 7933-7947.
- [128] R. Baron, N.M. Kershaw, T.J. Donohoe, R.G. Compton, *J. Phys. Org. Chem.*, 22 (2009) 1136-1141.
- [129] J.P. Bullock, E. Mashkina, A.M. Bond, *J. Phys. Chem. A*, 115 (2011) 6493-6502.
- [130] T.J. Dunn, L. Chiang, C.F. Ramogida, K. Hazin, M.I. Webb, M.J. Katz, T. Storr, *Chem. Eur. J.*, 19 (2013) 9606-9618.
- [131] Y.-W. Zhong, Z.-L. Gong, J.-Y. Shao, J. Yao, *Coord. Chem. Rev.*, 312 (2016) 22-40.
- [132] A. Hildebrandt, D. Miesel, H. Lang, *Coord. Chem. Rev.*, 371 (2018) 56-66.
- [133] R.F. Winter, *Organometallics*, 33 (2014) 4517-4536.
- [134] N. Segaud, E. Anxolabehere-Mallart, K. Senechal-David, L. Acosta-Rueda, M. Robert, F. Banse, *Chem. Sci.*, 6 (2015) 639-647.
- [135] G. De Leener, D. Over, C. Smet, D. Cornut, A.G. Porras-Gutierrez, I. Lopez, B. Douziech, N. Le Poul, F. Topic, K. Rissanen, Y. Le Mest, I. Jabin, O. Renaud, *Inorg. Chem.*, 56 (2017) 10971-10983.
- [136] A. Thibon-Pourret, F. Gennarini, R. David, J.A. Isaac, I. Lopez, G. Gellon, F. Molton, L. Wojcik, C. Philouze, D. Flot, Y. Le Mest, M. Reglier, N. Le Poul, H. Jamet, C. Belle, *Inorg. Chem.*, 57 (2018) 12364-12375.
- [137] M.G. Richmond, J.K. Kochi, *Inorg. Chem.*, 25 (1986) 656-665.
- [138] B. Gaš, J. Klíma, S. Záliš, A.A. Vlček, *J. Electroanal. Chem.*, 222 (1987) 161-171.
- [139] G.A. Heath, R.G. Raptis, *J. Am. Chem. Soc.*, 115 (1993) 3768-3769.
- [140] M.P. Cifuentes, M.G. Humphrey, G.A. Heath, *Inorg. Chim. Acta*, 259 (1997) 273-280.
- [141] J. Baldas, G.A. Heath, S.A. Macgregor, K.H. Moock, S.C. Nissen, R.G. Raptis, *J. Chem. Soc., Dalton Trans.*, (1998) 2303-2314.
- [142] A. M. Bond, P. J. Dyson, D. G. Humphrey, G. Lazarev, P. Suman, *J. Chem. Soc., Dalton Trans.*, (1999) 443-448.
- [143] M. Mlakar, S. Boulmaâz, H. Schönberg, H. Grützmacher, *Electroanalysis*, 15 (2003) 1043-1053.
- [144] W. Dai, S.B. Kim, R.D. Pike, C.L. Cahill, D.A. Sweigart, *Organometallics*, 29 (2010) 5173-5178.
- [145] Q. Zeng, M. Messaoudani, A. Vlček, F. Hartl, *Electrochim. Acta*, 110 (2013) 702-708.

- [146] D. Chong, V.H. Teixeira, M.J. Calhorda, W.E. Geiger, *Organometallics*, 33 (2014) 4706-4715.
- [147] M. Kawai, T. Yamaguchi, S. Masaoka, F. Tani, T. Kohzuma, L. Chiang, T. Storr, K. Mieda, T. Ogura, R.K. Szilagy, Y. Shimazaki, *Inorg. Chem.*, 53 (2014) 10195-10202.
- [148] J. Tory, G. Gobaille-Shaw, A.M. Chippindale, F. Hartl, *J. Organomet. Chem.*, 760 (2014) 30-41.
- [149] J. Tory, L. King, A. Maroulis, M. Haukka, M.J. Calhorda, F. Hartl, *Inorg. Chem.*, 53 (2014) 1382-1396.
- [150] L. Chiang, K. Herasymchuk, F. Thomas, T. Storr, *Inorg. Chem.*, 54 (2015) 5970-5980.
- [151] T.J. Del Castillo, N.B. Thompson, J.C. Peters, *J. Am. Chem. Soc.*, 138 (2016) 5341-5350.
- [152] J.O. Taylor, F.L.P. Veenstra, A.M. Chippindale, M.J. Calhorda, F. Hartl, *Organometallics*, 38 (2018) 1372-1390.
- [153] J.O. Taylor, G. Neri, L. Banerji, A.J. Cowan, F. Hartl, *Inorg. Chem.*, 59 (2020) 5564-5578.
- [154] B.D. Rossenaar, F. Hartl, D.J. Stufkens, C. Amatore, E. Maisonhaute, J.-N. Verpeaux, *Organometallics*, 16 (1997) 4675-4685.
- [155] S. Chardon-Noblat, Philippe D. Costa, A. Deronzier, T. Mahabiersing, F. Hartl, *Eur. J. Inorg. Chem.*, 2002 (2002) 2850-2856.
- [156] M. Busby, P. Matousek, M. Towrie, I.P. Clark, M. Motevalli, F. Hartl, A. Vlcek, Jr., *Inorg. Chem.*, 43 (2004) 4523-4530.
- [157] M. Górski, F. Hartl, T. Szymańska-Buzar, *Organometallics*, 26 (2007) 4066-4071.
- [158] S. Santi, L. Orian, C. Durante, A. Bisello, F. Benetollo, L. Crociani, P. Ganis, A. Ceccon, *Chem. Eur. J.*, 13 (2007) 1955-1968.
- [159] I.R. Corn, P.D. Astudillo-Sanchez, M.J. Zdilla, P.E. Fanwick, M.J. Shaw, J.T. Miller, D.H. Evans, M.M. Abu-Omar, *Inorg. Chem.*, 52 (2013) 5457-5463.
- [160] M. Bubrin, D. Schweinfurth, F. Ehret, S. Zálíš, H. Kvapilová, J. Fiedler, Q. Zeng, F. Hartl, W. Kaim, *Organometallics*, 33 (2014) 4973-4985.
- [161] S. Klod, K. Haubner, E. Jähne, L. Dunsch, *Chem. Sci.*, 1 (2010) 743-750.
- [162] K.D. Park, E.A. Muller, V. Kravtsov, P.M. Sass, J. Dreyer, J.M. Atkin, M.B. Raschke, *Nano Lett.*, 16 (2016) 479-487.
- [163] F. Miomandre, C. Allain, G. Clavier, J.-F. Audibert, R.B. Pansu, P. Audebert, F. Hartl, *Electrochem. Commun.*, 13 (2011) 574-577.
- [164] Y. Zhai, Z. Zhu, S. Zhou, C. Zhu, S. Dong, *Nanoscale*, 10 (2018) 3089-3111.

Electrochemistry and spectroelectrochemistry at low temperature

